# Using 222Rn to quantify wetlands interflow volume and quality discharging to headwater streams

K. Lefebvre, F. Barbecot, M. Larocque, Elisabeth Gibert-Brunet, M. Gillon, Aurélie Noret, C. Delbart

Applied Geochemistry 169 (2024) 106037

Contents lists available at ScienceDirect

Applied Geochemistry

journal homepage: www.elsevier.com/locate/apgeochem

# Using $^{222}$Rn to quantify wetlands interflow volume and quality discharging to headwater streams

K. Lefebvre [a,b,d,*], F. Barbecot [b], M. Larocque [b,c], E. Gibert-Brunet [d], M. Gillon [e], A. Noret [d], C. Delbart [f]

[a] Syndicat Mixte du Parc Naturel Régional de la Haute Vallée de Chevreuse, Chemin Jean Racine, 78640, Chevreuse, France
[b] GEOTOP Research Center, Université du Québec à Montréal, C.P. 8888 succursale Centre-ville, Montréal, H3C 3P8, Canada
[c] GRIL Research Center, Université du Québec à Montréal, C.P. 8888 succursale Centre-ville, Montréal, H3C 3P8, Canada
[d] UMR CNRS 8148-GEOPS, University of Paris Saclay, Rue du Belvédère, Bât. 504, 91405, Orsay, France
[e] UMR 1114-EMMAH, AU-INRAE, Avignon University, 301 rue Baruch de Spinoza, 84000, Avignon, France
[f] Université François Rabelais de Tours, EA 6293 GéHCO, Parc de Grandmont, 37200, Tours, France

ARTICLE INFO

Editorial handling by: D. Gooddy

*Keywords:*
Radon-222
Groundwater-surface water interaction
Interflow quantification
Riparian wetland
Headwater stream

ABSTRACT

Headwater streams are highly dependent on groundwater discharge to maintain low flows during dry periods and to dilute pollutants. Groundwater discharge to streams can have different flow paths, either from groundwater flowing directly to the river through the hyporheic zone or groundwater that emerges at the contact with a riparian wetland and flows mainly on the wetland surface. Differentiating these flows could be useful to assess the contribution of riparian wetlands in protecting stream water quality. The objective of this research was to expand the use of $^{222}$Rn as a groundwater tracer for small streams in headwater catchments to distinguish flows received directly from the aquifer and through riparian wetlands. $^{222}$Rn activities, phosphate ($PO_4^{3-}$) and nitrate ($NO_3^-$) concentrations, along with stream flows were used in a mass balance model to establish the proportions of groundwater flow that discharge to a small stream located southwest of the Paris Basin (France). This watershed is typical of headwater catchments in this region because it receives a wastewater treatment plant (WWTP) effluent at its source and its banks are occupied by many small riparian wetlands. To obtain the best accuracy of groundwater flow assessment, the field work was done during low flow conditions, where the stream flow was only 0.079 $m^3/s$ at the outlet. The model gives a good estimation of each flow path with 83 % of the stream baseflow originating from riparian wetlands. The large contrast in $^{222}$Rn activity between groundwater inflow from the aquifer (mean of 21 200 $Bq/m^3$) and interflows from wetlands (mean of 2310 $Bq/m^3$) renders the mass balance model sensitive to the separation of these two types of groundwater flow paths. At the head of the stream, water is characterized by high concentrations of $PO_4^{3-}$ and $NO_3^-$ due to the WWTP effluent into the stream (13 and 21 mg/L respectively). All groundwater flows are $PO_4^{3-}$ free and contribute to the improvement of stream water quality. The $NO_3^-$ cycle is more difficult to constrain because of the spatial heterogeneity in groundwater concentrations. Nevertheless, the results of the modeling approach showed that the main part of the evolution of $NO_3^-$ concentrations along the river can be explained by the dilution of stream flow with interflows. The method developed is considered sufficiently accurate to quantify groundwater inflows for different flow paths in headwater catchments and to estimate the impact of groundwater flow paths on stream water quality.

## 1. Introduction

In the last decades, numerous studies have focused on large rivers, mainly because human activities depend heavily on these water resources (Batlle-Aguilar et al., 2014a, b; Billen et al., 2007a; Schubert et al., 2020; Smerdon et al., 2012; Wang et al., 2015). In comparison, small streams in headwater catchments have received less attention, even though they can have an important impact on the quality and quantity of water in downstream rivers (Alexander et al., 2007; Fritz et al., 2018; Staponites et al., 2019; Wipfli et al., 2007) and on the nutrients cycles (Khamis et al., 2021; Marx et al., 2017; Van Stempvoort et al., 2022). Different criteria are used to define a watershed as a

* Corresponding author. Syndicat Mixte du Parc Naturel Régional de la Haute Vallée de Chevreuse, Chemin Jean Racine, 78640, Chevreuse, France.
*E-mail address:* lefebvre.karine@uqam.ca (K. Lefebvre).

https://doi.org/10.1016/j.apgeochem.2024.106037
Received 13 January 2024; Received in revised form 10 May 2024; Accepted 13 May 2024
Available online 21 May 2024

headwater catchment: the width of the channel (<1 m wide, Wipfli et al., 2007), the catchment area (<2 km$^2$; Horton, 1945 in Adams and Spotila, 2005), the hydromorphological context (area that is higher than the area where debris flows are deposited; Uchida et al., 2005), and the Strahler stream order (<3; Bieroza et al., 2024; Meyer et al., 2007). Using this last criterion, more than 75 % of linear rivers in France correspond to headwater streams, and their watersheds occupy more than 70 % of the country (Grivel and Caessteker, 2015). Due to their small size, the vulnerability of headwater streams to pollution events is generally high (Lane et al., 2022), especially where human activities are intensive (e.g., agricultural and urban areas). Due to their landscape position, stream flows from headwater catchments can be highly dependent on groundwater discharge (Molenat et al., 2008) and consequently playing a key role in diluting pollutants downstream, provided that it is not itself polluted. A better understanding of groundwater inflow to headwater streams is thus essential to manage water resources and to constrain pathways of nutrients and pollutants (Atkinson et al., 2015; Bieroza et al., 2024; Van Stempvoort et al., 2022).

Along the course of any given stream, the connections between surface water and groundwater can vary significantly in both space and time (Sophocleous, 2002). They can vary from the stream feeding the aquifer to the stream receiving water from groundwater inflow (Atkinson et al., 2015). In temperate climates, during low flow periods (*i.e.* when all temporary reservoirs are discharged), groundwater is often the only source of water for perennial stream (Winter, 1999), and thus controls the quality of stream water (Van Stempvoort et al., 2022). It is therefore important to quantify the spatiotemporal distribution of groundwater inflows to a river. Under temperate climates and in the presence of a permeable superficial aquifer, there is generally direct contact between the aquifer and the stream. Due to strong topographic gradients in headwater catchments (generally higher than 0.01, Gleeson et al., 2018), it is assumed that groundwater flows mainly from the aquifer to the stream and that flow from the stream to the aquifer is negligible. However, when the topography allows the development of riparian wetlands, the groundwater flow could be divided into three types of flows: (i) wetland seepage or groundwater overland flow, (ii) subsurface flow going through wetland sediments, and (iii) groundwater inflow from the aquifer through the streambed (Fig. 1). These flows can include a large range of groundwater transit times with different chemical composition. The distribution of these flows along a stream can also have a major impact on the quality of the stream water.

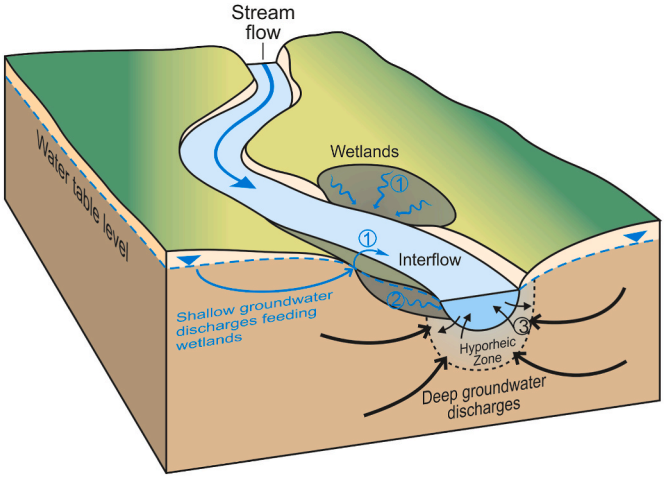


**Fig. 1.** Schematic representation of a stream sustained by different groundwater flow paths in a catchment where wetlands developed in riparian zones: interflows corresponding to the sum of (1) groundwater seepage or overland flow from wetlands to stream and (2) subsurface inflow from wetlands to stream, and groundwater inflow from the aquifer to the stream through the hyporheic zone (3) (Modified from Cook, 2013).

Over the past decades, many experiments have been carried out to quantify flows between groundwater and surface water, using physical, chemical, or isotopic methods. Physical methods based on Darcy's law (Landon et al., 2001) provide information on local flows in the vicinity of piezometers. But even in instrumented watersheds, estimations of hydraulic conductivities are often imprecise, adding to the uncertainty of the heterogeneity of groundwater inflows. In contrast, methods using tracers are integrative of all fluxes entering a stream section from all water reservoirs in the catchment. The quantification of groundwater inflows to the stream was attempted through the development of a wide array of tracers, including streambed water temperature (Becker et al., 2004; Briggs et al., 2012; Constantz, 2008; Dick et al., 2017), artificial tracers such as fluorescein or salt (Moore, 2004a, 2004b), natural tracers such as $^{222}$Rn (Adyasari et al., 2023; Avery et al., 2018; Batlle-Aguilar et al., 2014a, b; Cartwright and et Gilfedder, 2015; Cartwright et al., 2011; Cook et al., 2003; Lefebvre et al., 2015; Martinez et al., 2015), $\delta^{18}$O and $\delta^{2}$H (Meredith et al., 2009), $\delta^{13}$C (Meredith and Kuzara, 2012), and human-induced tracers such as $SF_6$ (Cook et al., 2006). $^{222}$Rn is often used to investigate groundwater – surface water interactions because it is inert, ubiquitous, and can be easily measured both on-site and in the laboratory (Adyasari et al., 2023; Dulaiova et al., 2005; Lefebvre et al., 2013). Moreover, $^{222}$Rn diffuses rapidly to the atmosphere when it reaches surface water, and a large gradient exists between groundwater and surface water end-members (Cable et al., 1996; Cook, 2013). It is a sensitive tool for the evaluation of groundwater discharge to rivers and streams (Atkins et al., 2016; Oh et al., 2021), even if uncertainties remain in estimating the degassing rate and the groundwater end-member activity (Adyasari et al., 2023; Zhou et al., 2024). The method generally used to estimate the degassing rate is to measure a second tracer in the stream to constrain the diffusion process such as $SF_6$ (Cook et al., 2006) or $\delta^{13}$C (Lefebvre et al., 2015). For the groundwater end-member characterization, most of studies used regional boreholes to sample groundwater and to estimate its $^{222}$Rn activity. The large range of activities in each aquifer illustrates the significance of uncertainty in groundwater inflow quantification (Adyasari et al., 2023). A way to reduce this uncertainty is to sample groundwater directly under the streambed.

The hyporheic zone is a transition zone between groundwater and stream water end-members for many geochemical tracers (Boulton et al., 2010; Winter et al., 1998). For the $^{222}$Rn, the hyporheic zone can be either a source (*i.e.* characterized by the production of $^{222}$Rn depending on sediment properties) or a sink (*i.e.* characterized by decay of $^{222}$Rn during the transfer of water through the sediments) in groundwater before it discharges to the stream. These processes have been documented in several studies (Batlle-Aguilar et al., 2014a, b; Cook et al., 2006). The hyporheic zone has been extensively studied over the last decade, because it is a highly reactive zone where water quality can be significantly altered (Boulton et al., 2010; Curie et al., 2009; Harvey et al., 2013; Peyrard et al., 2011; Schmadel et al., 2017).

Although floodplain wetlands connected to large rivers have been frequently studied (Billen et al., 2018; Fabre et al., 2020), few studies have focused on the role of small riparian wetlands in groundwater inflow quantity and quality in headwater catchments. However, it is widely recognized that wetlands are important to riparian ecosystems, providing habitats and food for a variety of species (Alard, 2002; Barnaud and Fustec, 2007). They often play a role in attenuating floods during high flows periods (Larocque et al., 2016; Tetzlaff et al., 2014) and in sustaining river flows during dry periods (Bullock and Acreman, 2003). In small rivers, riparian wetlands can also control the quality of groundwater before it discharges to rivers through biological activity, regulating $NO_3^-$ and $PO_4^{3-}$ content in water (Ranalli and Macalady, 2010; Walton et al., 2020). Thus, the quality of stream water can be affected by processes occurring in riparian wetlands (Kalin et al., 2012; Weyer et al., 2018). To assess this impact, the $NO_3^-$ and $PO_4^{3-}$ content can be used with a mass balance approach. This approach requires a spatial characterization of the groundwater and surface water chemistry and a

quantification of groundwater flux between the aquifer and the stream and between the wetlands and the stream.

The objectives of this research were (i) to expand the use of $^{222}Rn$ as a groundwater tracer for small streams in headwater catchments to distinguish groundwater flows received directly from the aquifer and from riparian wetlands (named interflows hereafter), and (ii) to characterize the impact of the groundwater flow paths to the stream quality. As a case study, the study focuses on a small headwater catchment located in France where there is a high density of riparian wetlands and an intensive human activity.

## 2. Study site

The study area is a small watershed of the Rhodon stream, located 15 km southwest of Paris in the Paris Basin (France). With a course of 10.5 km, the Rhodon stream is a headwater tributary of the Yvette River and drains a watershed of 26 $km^2$ (Fig. 2). It is located in the Natural Regional Park (*Parc naturel régional*) of the Haute Vallée de Chevreuse, within a watershed that has been the subject of a groundwater-wetland-stream interaction study by (Barbecot, 2006) and other studies helping to characterize groundwater in the Fontainebleau sand aquifer (Corcho Alvarado et al., 2007b, 2009; Gillon et al., 2009, 2012). Based on land cover data, the catchment is composed of 30 % agriculture, 19 % urban areas, 41 % forest, and 10 % meadow (Fig. 2a, European Union – SOeS, CORINE Land Cover, 2006; Büttner and Kosztra, 2007). Field crops (wheat, colza, and corn) dominate on plateaus and forests of deciduous trees, with oak-hornbeam forests and alder-beech forests prevail on hillslopes and in valleys. Wetlands are composed of grasslands and humid forests and cover 6,9 % of the catchment, mainly in the riparian zone of the stream. The main impact of urban areas on the water quality is from a wastewater treatment plant (WWTP) located at the stream head. Since its construction, the WWTP is the source of the stream and treats wastewater from 12 725 habitants (INSEE, 2015). Water treatment follows the classical steps, with filtration and oil-water separation phases followed by biochemical and chemical oxidation (through addition of $FeCl_3$). The WWTP effluents are monitored monthly and display a water chemistry dominated by dissolved organic carbon, ammonia, chloride, phosphate, and pesticides (WWTP administration, pers. comm.). However, the natural source of the stream sustained by the local groundwater is located between 1.5 km and 2 km downstream the WWTP (close to the sampling point S2, Fig. 2b). This characteristic is important to know, because along the first 2 km reach of the stream course, during low flows, the streamflow is only due to the WWTP effluents.

The climate throughout the study area is oceanic and temperate. The mean annual precipitation is 700 mm while the mean annual temperature is 10.5 °C (Météo_France, 2014). Recharge ranges ranging between 100 and 150 mm/yr and generally occurs between November and March (Corcho Alvarado et al., 2007a; Schneider, 2005).

The altitude of the catchment ranges from 78 to 165 m, and the altitudinal gradient varies from 0.18 for the left bank (northeastern hillslope) to 0.10 for the right bank (southwestern hillslope; Fig. 3). Plateaus dominate the catchment (68 %) while hillslopes and valleys cover 13 % and 19 % of the catchment area respectively. The geology of the site is composed by four sedimentary layers of the Paris Basin. With a mean thickness of 60 m and a saturated zone of approximately 40 m thick, the Fontainebleau sands aquifer sustains all streams of the upstream Yvette watershed (Rampon, 1965). The Fontainebleau sands aquifer is a well-known system on which many geochemical and hydraulic studies have been carried out (Bariteau, 1996; Corcho Alvarado et al., 2007a, 2009; Schneider, 2005). Composed of 99 % quartz, its hydraulic conductivity varies between $10^{-6}$ and $10^{-4}$ m/s (Schneider,

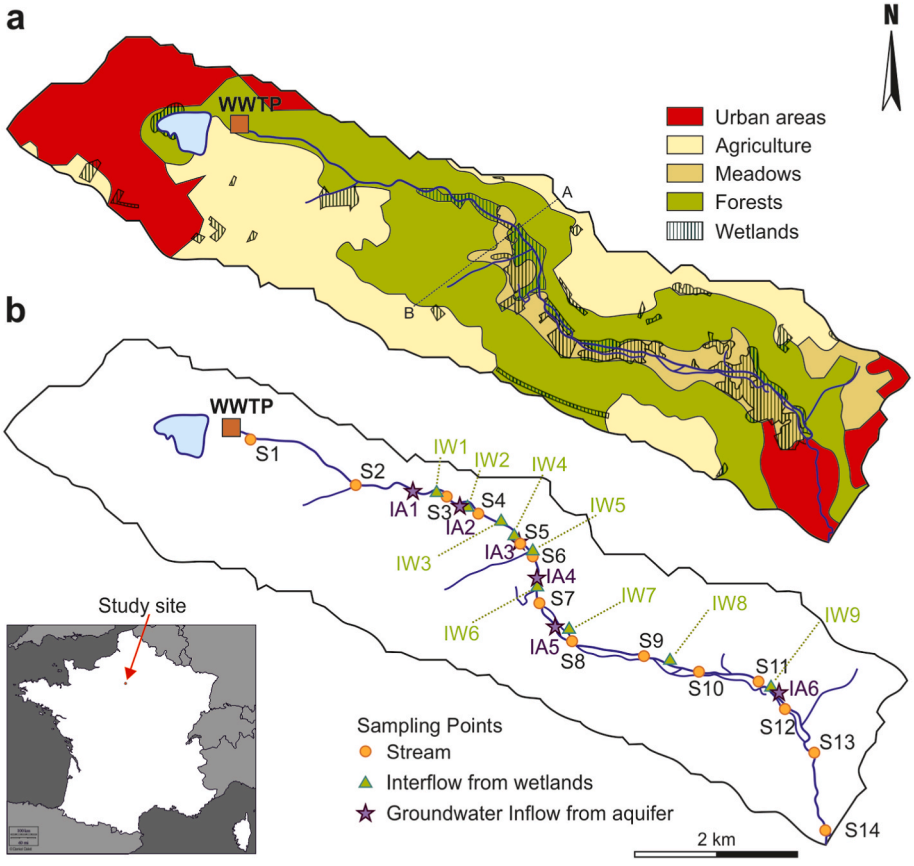


**Fig. 2.** Catchment of the Rhodon stream with (a) land use, and wetland coverage represented and (b) water sampling points; the dashed line corresponds to the cross section seen in Fig. 3. The outlet of the stream is characterized by the sampling point S14.

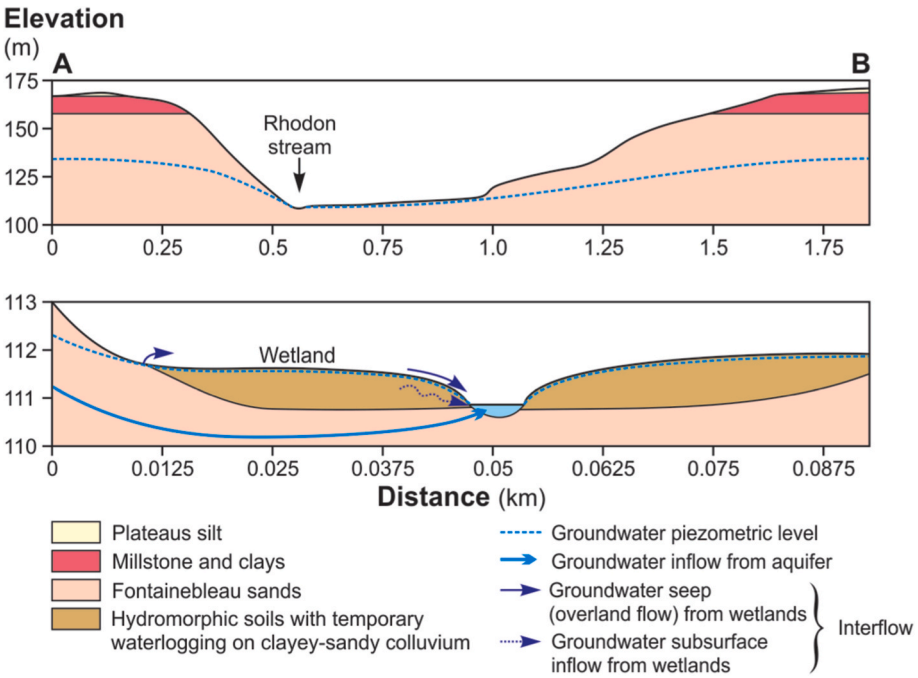


**Fig. 3.** Cross section of the Rhodon catchment with its geological context from the geological map 1/50 000 of Rambouillet (BRGM, 1975).

2005). Groundwater ages vary from a few years to 300–400 years (Corcho Alvarado et al., 2007b). The Fontainebleau sands are overlain by a thin layer of the altered Beauce Formation, composed of millstone and clay (Ménillet, 1988). Oligocene and Eocene marls form the lower boundary of the aquifer. In the valley, there is a heterogeneous layer of colluvium with low permeability on which small riparian wetlands are found. Along its course, the streambed lies on the Fontainebleau sands aquifer from 1.3 km to 7.5 km from the WWTP.

From 2.7 km downstream of the WWTP, along the course of the stream, evidence of groundwater seepage from springs sustaining the presence of riparian wetlands has been observed in 40 locations. These flows occur because of the break of slope between the hillsides and the valley, where groundwater flow is blocked by the low permeability of colluviums (Fig. 3). Most of these flows cannot be measured precisely because they are diffuse or have very low flow rates ($Q \leq 0.002$ m$^3$/s). Moreover, wetlands have been largely drained with numerous ditches since the 17th century due to the necessity to reduce the risks of disease associated with stagnant water in the valley. Nowadays, the riparian wetlands show many remnants ditches, which channel groundwater seepages. It is assumed here that inflows from wetlands, hereafter named interflows (IW), are linked to stream flow through these ditches.

The width of the Rhodon river varies between 1.3 and 3.7 m, whereas measured depths vary between 0.07 and 0.37 m. The average gradient of the streambed is 0.007. The annual mean flow rate at the outlet (S14, Fig. 2b) is 0.19 m$^3$/s (Lefebvre, 2015). At low flows, the mean flow rate is 0.070 m$^3$/s, mainly constituted by groundwater but including between 10 % and 20 % of water from the WWTP. The WWTP has a mean annual daily discharge of 0.022 m$^3$/s, decreasing between 0.010 and 0.016 m$^3$/s during low flows. The WWTP flows have a daily cycle, varying by ± 30 % around the daily mean value. The stream flow dynamic is classical for a temperate oceanic climate, with high flows during winter and low flows during the summer period (Fig. 4a). The system responds very quickly to precipitation events, and only 3–5 days are necessary for the streamflow to return to baseflow conditions (Fig. 4b), in accordance with the daily variations in baseflow due to the daily cycling of WWTP discharges. During the sampling campaign, the WWTP flow was only 0.006 m$^3$/s.

## 3. Material and methods

### 3.1. Field work and laboratory analyses

The field sampling campaign took place on the 8th and 9th September, 2014, during low flows after two weeks without any rain event (Fig. 4b). For this work, three types of water samples have been taken: (i) stream water at 14 stations (named S1 to S14; Fig. 2b), (ii) groundwater inflows from the aquifer in the streambed at six stations (named IA1 to IA6) and (iii) interflows at the outlet of the eight largest ditches flowing through riparian wetlands (with $Q < 0.004$ m$^3$/s, named IW1 to IW8).

Stream water was sampled on the first day. At each stream station, stream flow, $^{222}$Rn, pH, electrical conductivity (EC), and water temperature were measured on site, and water samples were taken for nutrients (nitrate and phosphate) and stable isotopes analyses in laboratory. Flow rates (Q) were measured with the velocity-area method using a micro-velocimeter (Sebahydrometrie; error between 5 and 10 %). EC (normalized at 25 °C), pH, and temperature were measured with portable electrodes (WTW 330i; error of 10 µS/cm, 0.05, and 0.1 °C respectively). $^{222}$Rn activity was measured with a portable Rad-7 counter, coupled with a Rad-Aqua degassing cell, produced by Durridge (Dulaiova et al., 2005). Each measure was integrated from 45 min of counting on a continuous pumping flow from the stream (pumping flow of 10.98 L/min), to achieve water-gas equilibrium and $^{222}$Rn-$^{218}$Po equilibrium. The errors vary between 5 % (for activities higher than 1000 Bq/m$^3$) and 17 % (for activities lower than 500 Bq/m$^3$), corresponding to 1σ standard variation. A pump (SDEC, 12V mini-twister pump) submerged in the middle of the stream section was used to measure $^{222}$Rn activities and to collect water samples in 10 mL glass bottles without headspace for $\delta^{18}$O and $\delta^{2}$H analyses, and in 60 mL Nalgene bottles for nutrients analyses.

Interflows were sampled on the second day. At the outlet of each ditch, the protocol described for the first day was used for pH, EC, temperature, stable isotopes, and nutrients. For the $^{222}$Rn measurements, due to small flows and supposed very low activities, we chose to sample water in 250 mL glass bottles and to send it to analyze to GEOTOP laboratory (UQAM) in Montreal (Canada). The discharge of these ditches was measured using the same method as the one used for stream

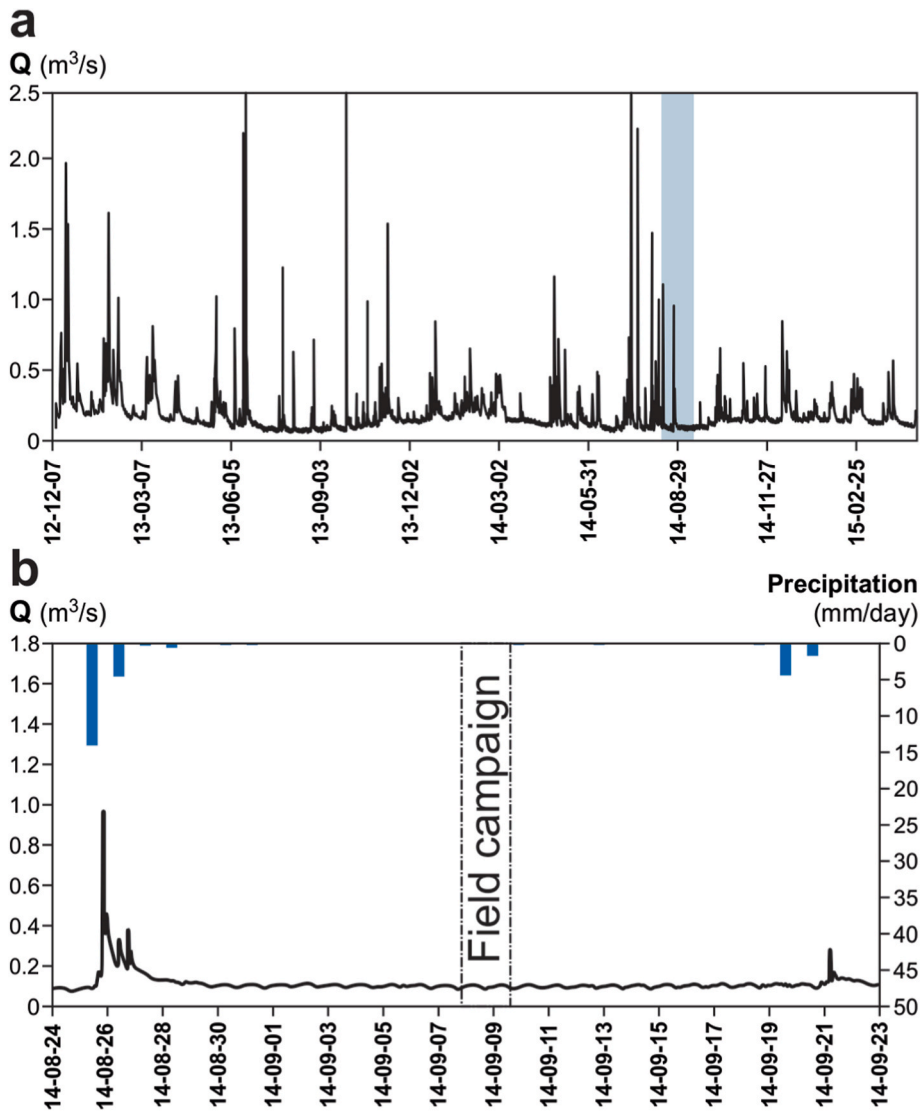


**Fig. 4.** Rhodon stream hydrograph at the outlet: (a) discharge from December 2012 to March 2015, and (b) precipitation and discharge during field work between August and September 2014.

flow whenever possible.

Groundwater inflows from the aquifer were also sampled on the second day. To constrain the $^{222}$Rn activity and chemistry of groundwater discharging through the hyporheic zone to the streambed, six ceramic cups (SDEC, model SPS 200) were installed at 1 m depth within the streambed in April 2014. Each ceramic cup allows to collect 500 mL of water. A small amount of that water was used in the field to measure pH, EC and temperature. The remaining water was sampled following the protocol described above for stable isotopes, nutrients, and $^{222}$Rn. All water samples for nutrients and water stable isotopes analyses were stored at 5 °C until analyses were performed.

$^{222}$Rn activity of groundwater inflows was measured by liquid scintillation counting (errors bars are equals to 1σ, Lefebvre et al., 2013) at the GEOTOP Laboratory (UQAM) in Montreal (Canada). $^{18}$O and $^{2}$H contents were measured with a Laser Water Isotope Analyzer (OA-ICOS, LGR DLT100) at the GEOPS laboratory (UPSaclay) in Orsay (France) and values are expressed as ‰ *vs* V-SMOW (Vienna Mean Ocean Water Standard; errors bars are equals to 0.2 ‰ for $\delta^{18}$O and 1 ‰ for $\delta^{2}$H). Nutrients concentrations ($NO_3^-$ and $PO_4^{3-}$) were measured by liquid chromatography (Dionex ICS-1000; error <10 %) at the GEOPS laboratory.

### 3.2. $^{222}$Rn modeling approach

#### 3.2.1. Modeling equation

In this study, the sampling campaign was organized to avoid any streamflow temporal variation focusing on (i) baseflow conditions to neglect all influence of rain event, and (ii) sampling following the mean transit time of the stream to neglect daily flow variation of the WWTP. Doing this ensured the steady state conditions necessary for modeling approach. The $^{222}$Rn mass balance model has been previously accurately constrained for large and small rivers using the following equation (Cook et al., 2006):

$$\frac{Q\partial c}{\partial x} = Ic_i + wEc - kwc - dw\lambda c + \frac{wh\theta(\gamma - \lambda c)}{1 + \lambda_{th}} \quad (1)$$

where $Q$ is the stream flow rate (m$^3$/day), $c$ is the radon activity within the stream (Bq/m), $x$ is the distance in the direction of flow (m), $c_i$ is the radon activity in groundwater (Bq/m), $I$ is the groundwater inflow per unit of river length (m$^2$/day), $w$ is the mean width of the stream (m), $E$ is the evaporation rate (m/day), $k$ is the gas transfer velocity of radon (m/day), $d$ is the mean depth of the stream (m), λ is the radioactive decay constant (day$^{-1}$), $h$ is the thickness of the hyporheic zone (m), $\theta$ is the porosity, $\gamma$ is the radon production rate within the hyporheic zone (Bq/

$m^3$/day), and $\lambda_{th}$ is the mean residence time in the hyporheic zone ($day^{-1}$).

In this study, evaporation and water fluxes from the hyporheic zone have been removed from the equation. Stream evaporation has been ignored, because this process is generally not significant in a temperate oceanic climate, with no wind during the sampling campaign. Because direct measurement of the evaporation rate couldn't be made on the field, stable isotopes of the water molecule were used to verify this assumption. This is consistent with the longitudinal evolution of the stable isotopes of water in the Rhodon stream, which does not show any evaporation trend, except for the samples corresponding to WWTP effluent, and the two wetland samples which have significant evaporated signatures (Fig. 5).

While in previous studies the possible $^{222}$Rn production in the direct groundwater inflow from the hyporheic zone was not measured *in situ* (Cook et al., 2006; McCallum et al., 2012), it is considered here through the use of specific sampling in ceramic cups within the river bed. The hyporheic zone contribution in terms of $^{222}$Rn is taken directly into account in the activity of the groundwater inflow from the aquifer ($c_{IA}$).

To represent interflows from wetlands, a new parameter was added to the equation. Therefore, groundwater flow from Eq. (1) was subdivided into inflows from the sand aquifer (IA) and interflows from wetlands (IW) (Eq. (2)).

$$\frac{Q\partial c}{\partial x} = q_{IA} * c_{IA} + q_{IW} * c_{IW} - \frac{D * w * c}{d_l} - dw\lambda c \quad (2)$$

where $q_{IA}$ is the groundwater inflow from the aquifer to the stream ($m^2$/s), $q_{IW}$ is the groundwater interflow from the wetlands ($m^2$/s), the sum of the $q_{IA}$ and $q_{IW}$ represents the total groundwater inflow to the stream ($I$), as measured during the sampling campaign, $c_{IA}$ is the radon activity in the groundwater inflow from the aquifer (measured in the streambed; Bq/m), $c_{IW}$ is the radon activity in the groundwater interflow from the wetlands (measured at the outlets of the largest ditches, represented by green triangles in Fig. 2b; Bq/m), $D$ is the diffusion coefficient of radon ($m^2$/s), and $d_l$ is the thickness of the diffusive layer (m).

Here, the gas transfer velocity, $k$, is replaced by the ratio $D/d_l$ to better constrain the degassing process. The parameter $k$ has a wide range of values depending on several parameters such as the diffusive coefficient of the gas considered ($D$), the wind velocity and the turbidity of the stream water. Since the $^{222}$Rn diffusive coefficient ($D$) is known for water temperatures from 0 °C to 30 °C (Broecker et Peng, 1974), it has been easily included in the equation. All other parameters influencing the degassing rate were considered in the thickness of the diffusive layer ($d_l$).

### 3.2.2. Parametrization and calibration

The sets of parameters and data used in the mass balance model are listed in Tables 1 and 2. $^{222}$Rn activity in the groundwater inflow from the aquifer endmember ($c_{IA}$) was estimated from the average of measurements done at different sites (purple stars in Fig. 2b). $^{222}$Rn activity in the groundwater interflows from wetlands has also been measured at several sites (green triangle in Fig. 2b), and the average value is used as $c_{IW}$. The thickness of the diffusive layer is set to $3.21 \times 10^{-5}$ m, which is the value already defined for a very similar small river of northern France (Lefebvre et al., 2015), which gives a gas transfer velocity consistent with other studies for headwater streams (Gleeson et al., 2018). The assumption behind this choice is that in similar climate, and stream dimensions ($Q$, $w$ and $d$ similar), the diffusive layer can be exported from one site to another. Finally, the stream is discretized into thirteen reaches determined by the sampling stream stations, which have been further discretized into 20 m subsections for calculation purposes.

Because both $q_{IA}$ and $q_{IW}$ are unknowns in Eq. (2), the calibration parameter α is related to the ratio of these two parameters for each stream segment (Eq. (3)).

$$\frac{q_{IA}}{q_{IW}} = \frac{\alpha}{1-\alpha} \quad (3)$$

It is assumed here that for each reach the stream flow gradient is linear and positive or 0. The model is calibrated to reproduce the longitudinal profiles of the total stream flow and $^{222}$Rn activity in the stream using the chi-square ($\chi^2$) as a calibration objective of the SOLVER inversion tool in EXCEL (Eq. (4)).

$$\chi^2 = \sum \frac{(Am - As)^2}{e} \quad (4)$$

where $A_m$ is the measured $^{222}$Rn activity in the stream ($Bq/m^3$), $A_s$ is the simulated $^{222}$Rn activity in the stream ($Bq/m^3$), and $e$ is the standard error of the measurement ($Bq/m^3$).

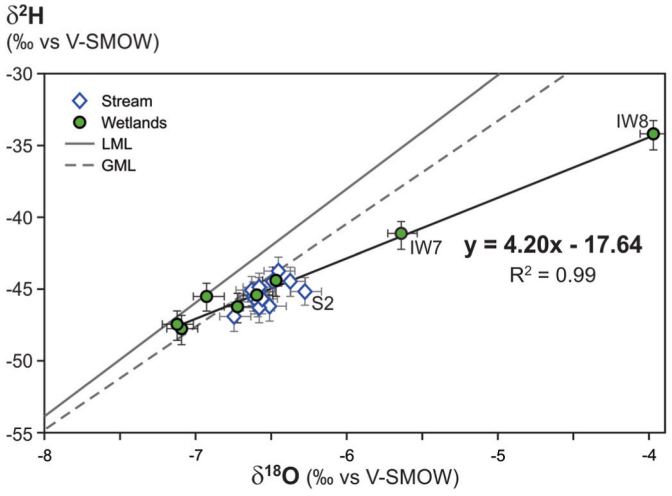


**Fig. 5.** Isotopic compositions of stream water and wetland water. Error bars correspond to the analytical uncertainty at 1σ. The purple line corresponds to the evaporation trend of the wetland samples. The global meteoric line (black line) is defined by Craig's equation (Craig, 1957), whereas the local meteoric line (dashed black line) has been obtained from 12 years of fortnightly data collect at the GEOPS laboratory (Barbecot F., pers. Comm).

**Table 1**
Model Parametrization for the $^{222}$Rn mass balance.

| Parameter | Symbol | Value | Units | Source of data |
|---|---|---|---|---|
| **Imput parameters** | | | | |
| A$^{222}$Rn of groundwater flow from aquifer | $c_{IA}$ | 21 200 | Bq/$m^3$ | *calculated as the mean of the measurements* |
| A$^{222}$Rn of interflow | $c_{IW}$ | 2310 | Bq/$m^3$ | *calculated as the mean of the measurements* |
| Diffusion coefficient of$^{222}$Rn | $D$ | $1.10 \times 10^{-9}$ | $m^2$/s | *from Broecker and Peng (1974)* |
| A$^{222}$Rn of the atmosphere | $c_a$ | 0 | Bq/$m^3$ | *from Cook et al. (2003)* |
| Thickness of the diffusive layer | $d_l$ | $3.21 \times 10^{-5}$ | m | *from Lefebvre et al. (2015)* |
| River width | $w$ | see Table 2 | m | *measured on the field* |
| River depth | $d$ | see Table 2 | m | *measured on the field* |
| Radioactive decay constant of$^{222}$Rn | $\lambda$ | $2.09 \times 10^{-6}$ | $s^{-1}$ | |
| **Parameters estimated by the model** | | | | |
| Groundwater inflow from aquifer | $q_{IA}$ | | $m^3$/s | *optimized by the model* |
| Groundwater interflow from wetlands | $q_{IW}$ | | $m^3$/s | *optimized by the model* |
| Ratio between inflow and interflow | $\alpha$ | | | *calibration parameter* |

**Table 2**
Physio-chemical measurements of the sampled stream sites.

| ID | Distance from the spring | pH | CE (norm. 25 °C) | Temp. | Q | $^{222}$Rn | $NO_3^-$ | $PO_4^{3-}$ | $\delta^2H$ | $\delta^{18}O$ | w | d |
|---|---|---|---|---|---|---|---|---|---|---|---|---|
| | km | | µS/cm | °C | $m^3/s$ | Bq/$m^3$ | mg/L | | ‰ | | m | m |
| S1 | 0 | 7.8 | 1249 | 20.3 | 0.006 | 0 | 12 | 13 | −45.2 | −6.3 | 1.8 | 0.17 |
| S2 | 1.5 | 8.3 | 1230 | 17.6 | 0.004 | 0 | 21 | 12 | −43.8 | −6.4 | 1.9 | 0.13 |
| S3 | 2.7 | 7.9 | 1067 | 15.4 | 0.010 | 1400 | 22 | 11 | −44.5 | −6.5 | 1.3 | 0.08 |
| S4 | 3.4 | 7.7 | 814 | 14.5 | 0.013 | 2310 | 19 | 7 | −45.6 | −6.6 | 1.3 | 0.37 |
| S5 | 4.0 | 7.7 | 737 | 15.3 | 0.036 | 1780 | 21 | 0 | −44.5 | −6.4 | 2.0 | 0.19 |
| S6 | 4.3 | 8.0 | 735 | 15.4 | 0.034 | 809 | 23 | 2 | −46.3 | −6.5 | 1.9 | 0.07 |
| S7 | 4.9 | 8.0 | 707 | 15.8 | 0.051 | 496 | 19 | 0 | −45.8 | −6.6 | 1.3 | 0.11 |
| S8 | 5.6 | 8.1 | 708 | 16.8 | 0.046 | 377 | 21 | 3 | −47.0 | −6.7 | 1.9 | 0.25 |
| S9 | 6.4 | 8.0 | 698 | 16.9 | 0.041 | 335 | 19 | 0 | −46.0 | −6.6 | 2.9 | 0.18 |
| S10 | 7.3 | 8.1 | 696 | 17.5 | 0.048 | 297 | 18 | 0 | −46.4 | −6.6 | 2.8 | 0.25 |
| S11 | 8.0 | 8.0 | 693 | 17.7 | 0.042 | 267 | 17 | 0 | −45.2 | −6.6 | 2.5 | 0.37 |
| S12 | 8.5 | 8.1 | 696 | 17.8 | 0.049 | 306 | 17 | 0 | −45.1 | −6.6 | 2.1 | 0.27 |
| S13 | 9.3 | 8.1 | 701 | 17.7 | 0.066 | 120 | 17 | 0 | −45.8 | −6.6 | 3.7 | 0.13 |
| S14 | 10.5 | 8.2 | 711 | 17.5 | 0.079 | 223 | 19 | 0 | −44.9 | −6.6 | 2.8 | 0.19 |

#### 3.2.3. Sensitivity analysis

From previous studies, the main parameters which can have a significant impact on the quantification of fluxes are the $^{222}$Rn activities in the aquifer, and the diffusion process (Cartwright and et Gilfedder, 2015; Cartwright et al., 2011; Cook, 2013; Stellato et al., 2008). A sensitivity analysis of the model to variations in the $c_{IA}$, $c_{IW}$, and $d_l$ parameters was performed with different combinations of the parameters to evaluate the efficiency of the set of selected parameters. $c_{IA}$ and $c_{IW}$ have been tested in the natural range of activities found on the field, and the thickness of the diffusive layer was tested in a range from −50 % to +50 % around the best-fit value. The stream characteristics such as streamflow *(Q)*, depth *(d)* and width *(w)* could also add some uncertainty on the results of the model. In this study site, the rectification of the stream bed resulted in only small variations of *w* and *d*, so the assumption was made that they were not significant for this approach. As for the streamflow, the impact could be significant on the total flows (*i.e.* the sum of interflows and groundwater inflow), but not really on the distribution of inflows between the aquifer and the wetlands, so it was not considered in the sensitivity analysis.

### 3.3. $NO_3^-$ and $PO_4^{3-}$ dynamics in the stream

In the stream, the evolution of nutrients concentrations can be due to (i) groundwater inflow from the aquifer, (ii) groundwater interflow from wetlands, and (iii) biochemical processes in the stream. The groundwater inflow repartition between the aquifer and the wetlands, obtained using $^{222}$Rn modeling approach, allows to quantify the nutrients mass reaching the stream. To calculate these amounts for each reach, a mass balance approach was used (Eq. (5)).

$$Cn_{(x)}Q_{(x)} = Cn_{(x-1)}Q_{(x-1)} + Cn_{IA}Q_{IA(x)} + Cn_{IW}Q_{IW(x)} \quad (5)$$

where $Cn_{(x)}$ is the nutrient concentration ($NO_3^-$ or $PO_4^{3-}$) in the stream at the end of the reach x, $Q_{(x)}$ is the stream flow at the end of the reach x ($m^3/s$), $Cn_{(x-1)}$ is the nutrients concentration in the stream at the end of the reach x-1 (mg/L), $Q_{(x-1)}$ is the stream flow at the end of the reach x-1 ($m^3/s$), $Cn_{IA}$ is the mean of nutrient concentration in the groundwater inflow from the aquifer (mg/L), $Q_{IA(x)}$ is the groundwater inflow from the aquifer along the reach x ($m^3/s$), $Cn_{IW}$ is the mean of nutrients concentration in the groundwater inflow from the wetlands (mg/L), $Q_{IW(x)}$ is the groundwater inflow from the wetlands along the reach x ($m^3/s$).

For a given reach, the relationships between $q_{IA}$ and $Q_{IA}$ and between $q_{IW}$ and $Q_{IW}$ are described as follows:

$$Q_{IA} = q_{IA} * L \quad (6)$$

$$Q_{IW} = q_{IW} * L \quad (7)$$

where L is the length of the reach.

The chemistry of the groundwater endmember *($Cn_{IA}$)* and of the interflow from wetlands endmember *($Cn_{IW}$)* were calculated as means of the measurements on IA samples and IW samples respectively. It is assumed that the impact of biochemical processes can be estimated by quantifying the difference between the nutrient's concentrations in the stream and the nutrient concentrations calculated with the mass balance approach.

## 4. Results

### 4.1. Water endmembers chemistry and flows

In the catchment, three end members of water that mix in the stream have been identified: (i) the WWTP effluent at the spring, (ii) the groundwater inflow from the aquifer and (iii) the interflow from the wetlands. The WWTP effluents are characterized by the S1 results (Fig. 6, Table 2), showing that the water has no $^{222}$Rn activity, pH of 7.8, high electrical conductivity (1249 µS/cm), high temperature (20.3 °C) and high $PO_4^{3-}$ concentration (13 mg/L). Groundwater flows from the aquifer have a large range of $^{222}$Rn activities, from 13 180 to 35 474 Bq/$m^3$ with a mean of 21 200 Bq/$m^3$ (Table 3). Electrical conductivity is less variable, ranging from 511 to 634 µS/cm, and pH is generally lower than the other endmembers, ranging from 7.1 to 7.9. Except the IA4 sample, no samples contain phosphates. For nitrates, two groups are distinguished. The first group has high nitrates concentrations (between 23 and 28 mg/L) and corresponds to the section between 2.6 and 2.9 km from the spring. The second group has low nitrates concentrations (0–5 mg/L) and corresponds to the section between 3 km from the spring and the outlet. In the third influx, the interflows from wetlands have low $^{222}$Rn activities (200–5800 Bq/$m^3$, Table 3), with a mean of 2310 Bq/$m^3$. The pH is mainly higher than groundwater inflows (7.3–8.6), but the electrical conductivity is similar for the two other types of flows (528-708 µS/cm for interflows). No phosphates were found for interflows samples, but a large range of nitrates were found (4–41 mg/L), with lowest concentrations in the second half-part of the stream, between 5.6 km from the spring and the outlet, and highest concentrations in the medium section, between 3,8 and 4.4 km from the spring. With only 0.004–0.006 $m^3/s$, the WWTP input accounts for around 5–8 % of the total stream flow. The five largest ditches going through wetlands that can be measured *in situ* present flows between 0.001 and 0.003 $m^3/s$ (Table 3).

### 4.2. Flow rates, water chemistry, and $^{222}$Rn activity in the stream

From the spring to the outlet, stream flow increases from 0.006 $m^3/s$ to 0.079 $m^3/s$ (Fig. 6a–Table 2). The stream flow measurements show

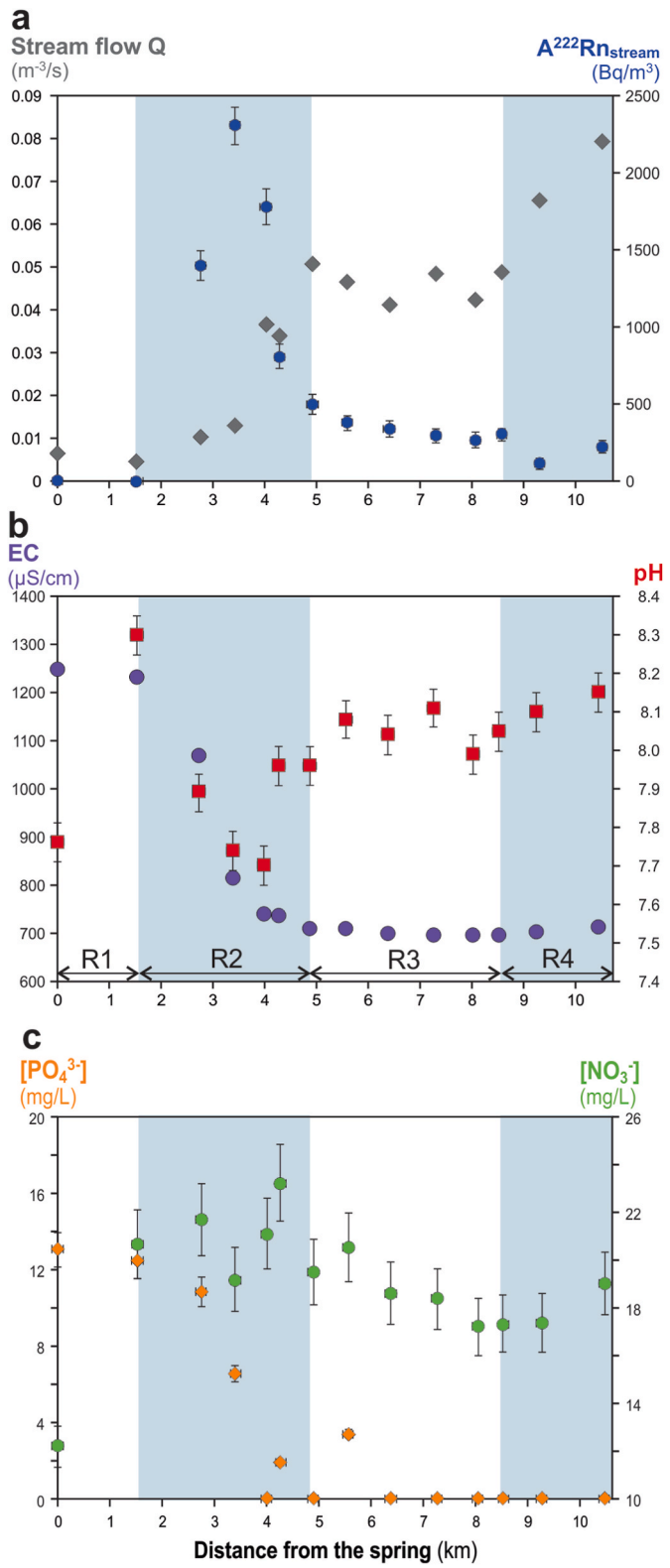


**Fig. 6.** Longitudinal profiles of (a) stream flow (grey diamonds) and $^{222}$Rn activity in the stream (deep blue circles), (b) the electrical conductivity (purple circles) and the pH (red squares) of stream water, and (c) nitrate (green circles) and phosphate (orange diamonds) concentrations in the stream as a function of the distance from the spring. Blue boxes correspond to the most substantial groundwater contribution areas (R2 and R4).

two sections with no significant variations: between the spring and 1.5 km downstream, and between 4.9 km and 8.5 km from the spring. There are also two majors gaining areas along the stream: between 1.5 and 4.9 km, marked by an increase of the stream flow from 0.004 to 0.036 $m^3/s$ and between 8.5 and 10.5 km, with the stream flow increasing from 0.049 to 0.079 $m^3/s$. The stream course can be divided in 4 reaches: R1 (0–1.5 km), R2 (1.5–4.9 km), R3 (4.9–8.0 km) and R4 (8.0–10.5 km).

R1 is characterized by high electrical conductivity (1230-1249 µS/cm), no $^{222}$Rn activity, high $PO_4^{3-}$ concentrations (12–13 mg/L) and increases in pH and $NO_3^-$ concentrations (from 7.8 to 8.3 and from 12 to 21 mg/L, respectively).

R2 is characterized by a major decrease in EC and $PO_4^{3-}$ concentrations (from 1230 to 707 µS/cm and from 12 to 0 mg/L, respectively), a peak of $^{222}$Rn up to 2310 Bq/$m^3$ at 3.4 km, followed by a decrease of the activities down to 496 Bq/$m^3$. The pH decreases from 8.3 to 7.7 at 4.0 km and then increases again to 8.0. In this reach no significant evolution in $NO_3^-$ concentrations is observed.

R3 is characterized by no significant evolution in EC (mean of 699 µS/cm), pH (mean of 8.1), $^{222}$Rn (mean of 320 Bq/$m^3$) and $PO_4^{3-}$ concentrations (0 mg/L, except for one sample). Only $NO_3^-$ concentrations present a small decrease in the stream (from 21 to 17 mg/L). The plateau observed in pH value illustrates an equilibration of stream water inorganic carbon with the atmosphere (Lefebvre et al., 2015).

R4 is characterized by no significant evolution in EC (mean of 706 µS/cm), pH (mean of 8.1), $PO_4^{3-}$ (mean of 0), $NO_3$ (mean of 18 mg/L) and a small decrease in $^{222}$Rn activities (from 306 to 223 Bq/$m^3$).

### 4.3. Modeling results

#### 4.3.1. $^{222}$Rn dynamic and distribution of inflows between groundwater from aquifer and interflow from wetlands

With the input parameters presented in Table 1, $q_{IA}$ and $q_{IW}$ were estimated for each section to obtain the best simulation of $^{222}$Rn activity in stream water (corresponding to a $\chi^2$ of 1042). Along the stream, the contribution of the groundwater inflowing as interflows from the riparian wetlands is about 79 % whereas the groundwater inflowing from the aquifer contributes to 21 % of the streamflow (Fig. 7a–b). In R1, there is no contribution of groundwater. In R2, the first contributing reach, a rapid dilution of the WWTP effluent is observed by the groundwater inflows. But this contribution evolves inside the reach. Between 2.7 and 3.3 km from the spring, 66 % of the groundwater inflow comes from the aquifer and 34 % comes from wetlands interflows. This is sustained by the direct connection between the aquifer and the streambed observed on the geological map (BRGM, 1975). However, changes occur rapidly at the end of the reach (after 3.3 km), with interflows from wetlands becoming dominant (85 % of inflows to the stream) and inflows from the aquifer contributing only for 15 %. In R3, interflows still dominate the very low increase of stream flow. In R4, between 8.5 and 10.5 km, 93 % of groundwater discharge to the stream comes from interflows. In this area, where the Rhodon flows on clays and marls sediments, the Fontainebleau sand feeds the wetlands that carry groundwater to the river and contributes for the last increase of streamflow, marked by a decrease of $^{222}$Rn activities.

#### 4.3.2. $NO_3^-$ and $PO_4^{3-}$ dynamics

To reproduce the $PO_4^{3-}$ evolution in the stream, the mass balance was made with an aquifer endmember ($Cn_{IA}$) and an interflow from wetlands endmember ($Cn_{IW}$) at 0 mg/L. To reproduce the $NO_3^-$ evolution in the stream, the mass balance was made with a wetland endmember ($Cn_{IW}$) obtained by the mean of the eight samples reported in Table 3. For the aquifer endmember ($Cn_{IA}$), it was separate in two groups to follow the distribution of groundwater chemistry identified in the IA samples: the first one corresponding to the mean of IA1 and IA2 sampling points (25.5 mg/L), used for the stream mass balance at the beginning of the R2 (until 3 km from the spring) and the second one corresponding to the mean of IA3 to IA6 (3.25 mg/L), used for the mass balance for the rest of

**Table 3**
Physio-chemical measurements of sampled groundwater inflows from the aquifer and interflows from the wetlands.

| ID | Distance from the spring | pH | CE (norm. 25 °C) | Temp. | Q | $^{222}$Rn | $NO_3^-$ | $PO_4^{3-}$ | $\delta^2$H | $\delta^{18}$O |
|---|---|---|---|---|---|---|---|---|---|---|
| | km | | µS/cm | °C | $m^3/s$ | $Bq/m^3$ | mg/L | | ‰ | |
| IW1 | 2.7 | 8.1 | 695 | 14.6 | n.d | 200 | 15 | 0 | −47.9 | −7.1 |
| IW2 | 3.1 | 7.4 | 534 | 12.1 | 0.001 | 7800 | 23 | 0 | −45.6 | −6.9 |
| IW3 | 3.7 | 7.7 | 708 | 15.9 | 0.002 | 2800 | 20 | 0 | −44.5 | −6.5 |
| IW4 | 3.8 | 8.0 | 626 | 14 | n.d | n.d | 30 | 0 | −46.4 | −6.7 |
| IW5 | 4.0 | 8.1 | 599 | 13.2 | 0.002 | 300 | 41 | 0 | −45.6 | −6.6 |
| IW6 | 4.4 | 7.3 | 639 | 12.7 | n.d | 5700 | 28 | 0 | −47.6 | −7.1 |
| IW7 | 5.6 | 8.5 | 528 | 21.3 | 0.001 | 500 | 4 | 0 | −41.3 | −5.6 |
| IW8 | 6.3 | 8.6 | 573 | 22.4 | 0.003 | 400 | 6 | 0 | −34.3 | −4.0 |
| IA1 | 2.6 | 7.8 | 535 | 12.1 | n.d | 16 475 | 23 | 0 | −46.3 | −6.5 |
| IA2 | 2.9 | 7.9 | 602 | 13.5 | n.d | 35 474 | 28 | 0 | −42.1 | −5.8 |
| IA3 | 3.2 | 7.1 | 511 | 15.5 | n.d | 20 864 | 0 | 0 | −49.1 | −7.3 |
| IA4 | 4.3 | 7.6 | 560 | 15.8 | n.d | 19 739 | 4 | 4 | −49.8 | −7.2 |
| IA5 | 4.7 | 7.2 | 542 | 13.5 | n.d | 21 366 | 5 | 0 | −46.6 | −7.0 |
| IA6 | 7.9 | 7.8 | 634 | 15.2 | n.d | 13 180 | 4 | 0 | −50.2 | −7.3 |

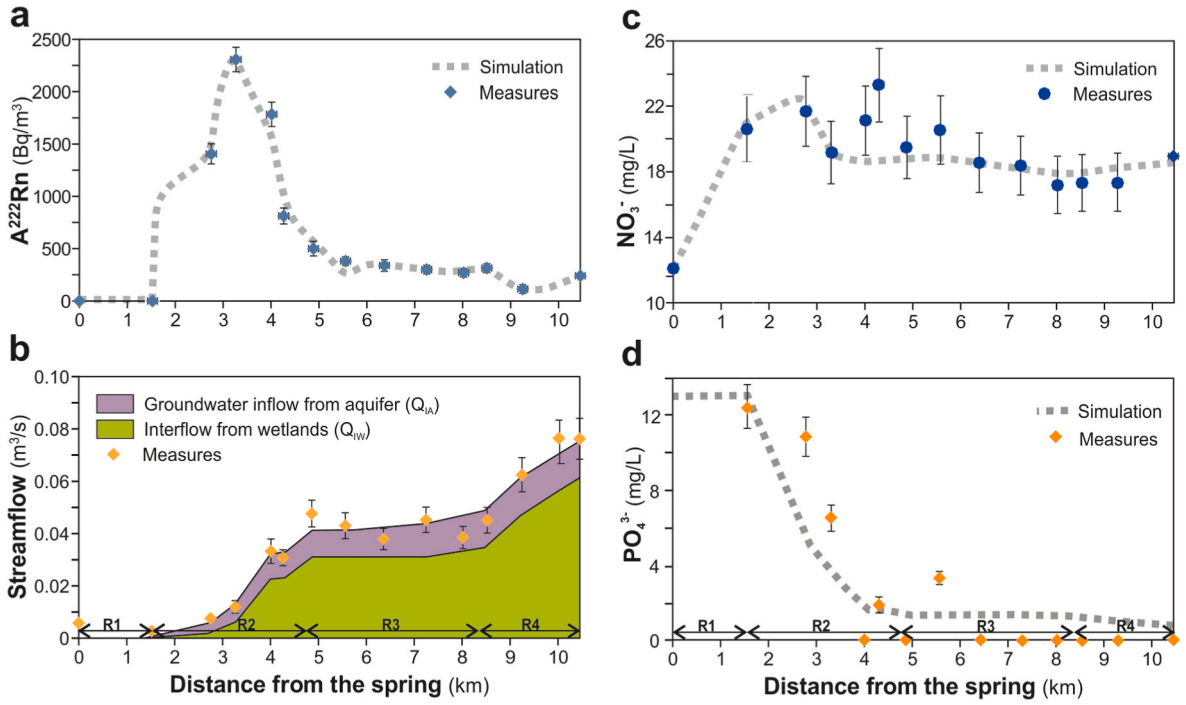


**Fig. 7.** Measured and simulated $^{222}$Rn activities along the stream (a), measured flow rates, with modeled groundwater contribution from the aquifer to the stream and interflow from wetlands (b), measured and simulated $NO_3^-$ concentrations along the stream (c) and measured and simulated $PO_4^{3-}$ concentrations along the stream (d). Error bars represent 1σ error from the analytical and field methods.

the stream course.

The mass balance approach gives a good illustration of the nutrient dynamics (Fig. 7c–d). The trends are well represented all along the stream course for the two nutrients. The $NO_3^-$ concentrations are somewhat underestimated between 3.5 and 6 km. From 3.5 to 4.5 km, the flow gain in the stream is mainly due to interflows from wetlands (IW4, IW5 and IW6), which contain more $NO_3^-$ than other interflows from wetlands, so the mean used for the modeling approach could underestimate the contribution of wetlands flows in this part. This can explain the difference between simulation and observation. The underestimation of $PO_4^{3-}$ concentrations occurs where the groundwater inflow comes mainly from the aquifer through the streambed. The sensitivity of this tracer is lower than for $NO_3^-$, due to the analytical method that cannot measure concentrations <1 mg/L. The mass balance approach highlighted that no significant mark of biochemical processes occurred along the Rhodon stream.

## 5. Discussion

### 5.1. Model sensitivity to $^{222}$Rn activities and diffusion process

To determine the sensitivity of the model to its parameters, simulations were repeated for different values of $c_{IA}$, and $c_{IW}$, considering a constant total groundwater inflow (*i.e.* the sum of $q_{IA}$ and $q_{IW}$). These variables were changed manually one at a time, to reproduce the range of $^{222}$Rn activities found in the catchment. The $\chi^2$ was recalculated for each variation of the two parameters following model optimization. The results are presented in Fig. 8.

This analysis shows a significant impact of the estimation of $c_{IA}$ on the quantification of fluxes, with a variation of 0.02 $m^3/s$ between the lowest and the highest activity used for the groundwater from aquifer endmember (Fig. 8a). On the contrary, the change in the $^{222}$Rn activity for the interflow endmember ($c_{IW}$) seems to have no impact on the quantification of flows (Fig. 8b). Because the $c_{IW}$ parameter is almost ten

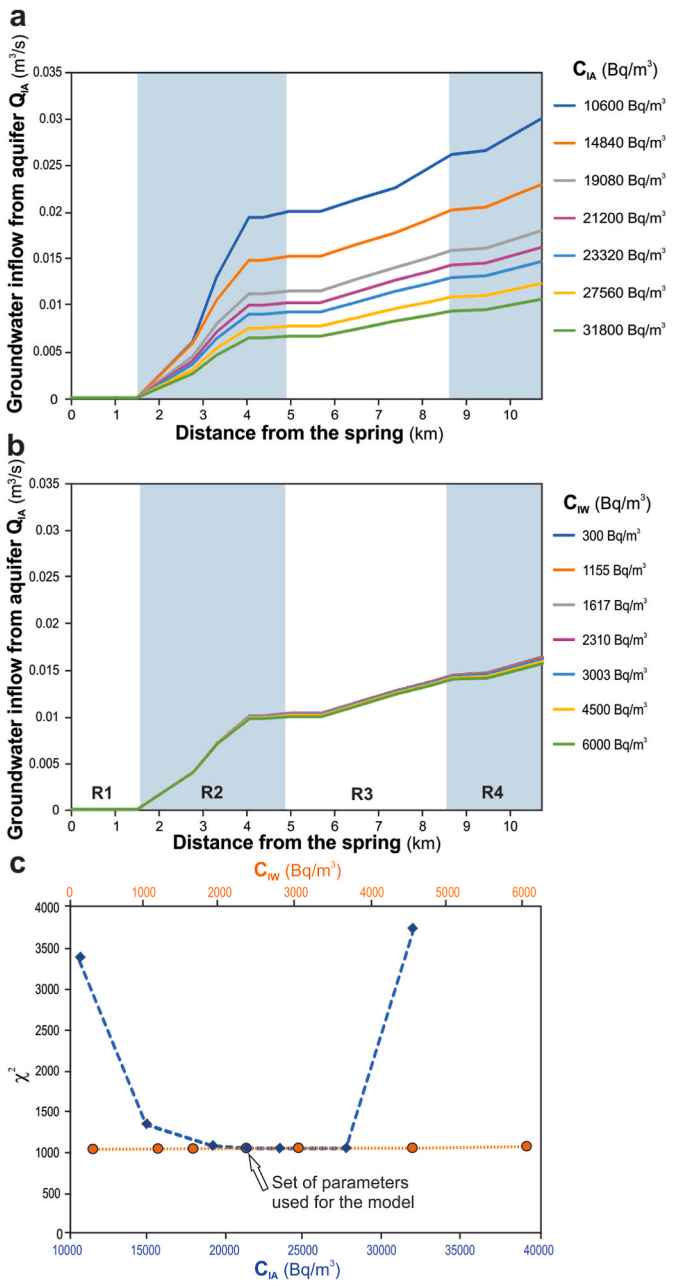


**Fig. 8.** Sensitivity analysis of the model on the endmembers activities in $^{222}$Rn: (a) evolution of the groundwater inflow from the aquifer ($q_{IA}$) with respect to the variation of $c_{IA}$, (b) evolution of the groundwater inflow from the aquifer ($q_{IA}$) with respect to the variation of $c_{IW}$, and (c) evolution of the $\chi^2$ parameter calculated for each variation of $c_{IA}$ and $c_{IW}$.

times smaller than $c_{IA}$ ($c_{IA}/c_{IW} = 9.18$), varying $c_{IW}$ in the natural range found in the catchment couldn't have a significant impact on the model. This is true even though the total inflow from the aquifer through the hyporheic zone flow is much smaller than the one of the wetlands' surface interflows. From the measurements on the ceramic cup samples, $c_{IA}$ has been found to vary between −50 % and +50 % around the mean value used in the model. This range of $c_{IA}$ variation could induce a variation between −50 % and +100 % of the $q_{IA}$ estimation, corresponding to a contribution of $q_{IA}$ to the total stream flow comprised between 12.7 % and 38 %. The reliability in the values used for the current model is ensured by the $\chi^2$ value, which is minimized when the $c_{IA}$ equals the mean of the values found in the catchment (Fig. 8c). Considering that the $\chi^2$ is constant for $c_{IA}$ between 19 080 Bq/m3 and 31 800 Bq/$m^3$, the uncertainty on the contribution of groundwater from aquifer is comprised between 0.010 and 0.017 $m^3$/s, corresponding to 0.015 ± 0.005 $m^3$/s. Thereby, the groundwater from wetlands contribution varies from 0.057 to 0.064 $m^3$/s around the best fit value of 0.059 $m^3$/s. Based on these elements, the uncertainty of the model is about ±6 %.

Another source of uncertainty is the thickness of the diffusive layer. Here, the value chosen for the model was taken from a precedent study (Lefebvre et al., 2015). The modeling approach was tested for different values around the chosen one, and the results sustain that the model is sensitive to this parameter, in the same way than for the $c_{IA}$ value (Fig. 9). The contribution of groundwater inflow from aquifer to the stream could vary from 39 % for the smallest value of $d_l$ to 12 % for the highest value of $d_l$. The best-fit modeling results, corresponding to the minimal $\chi^2$, is found for the $d_l$ determined in the previous study.

From this sensitivity analysis, it appears that (i) the modeling approach is not sensitive to $c_{IW}$ variations, (ii) the modeling approach is very sensitive to $c_{IA}$ and $d_l$ variations, (iii) a fluctuation of 50 % in $c_{IA}$ or in $d_l$ generates between 8 % and 19 % of variation in the contribution of groundwater inflow from the aquifer ($q_{IA}$), and (iv) the best fit model corresponds to the set of parameter chosen for the modeling approach and presented in Table 1.

### 5.2. *Link between groundwater flow paths and the quality of stream water*

Along the stream, two sections can be observed: (i) R1, where EC and $PO_4^{3-}$ are constant and pH and $NO_3^-$ increase (Fig. 6), and (ii) the rest of the stream where the water quality clearly improved (Figs. 6 and 7). In R1, because no inflow is observed in this reach, the evolution of pH and $NO_3^-$ could only be due to chemical process in the stream water. The increase of pH illustrates the equilibration of the inorganic carbon in water with the atmosphere (by degassing process), whereas the increase of $NO_3^-$ could be explained by an oxidation of $NH_4^+$ into $NO_3^-$, as this process can be observed downstream WWTP discharges (Haggard et al., 2005; Marti et al., 2004). From R2 to R4, although the WWTP effluent at the spring is generally enriched in both $PO_4^{3-}$ and nitrogen compounds ($NH_4^+$ and $NO_3^-$), the combination of groundwater inflow from the aquifer and groundwater flowing as interflows through the riparian wetlands allows for a rapid dilution of $PO_4^{3-}$, and a less marked dilution of $NO_3^-$. Analytical results of groundwater inflow from the aquifer and interflow from wetlands samples show that neither of these flows has $PO_4^{3-}$ loads above the detection limit (*i.e.* all concentrations were

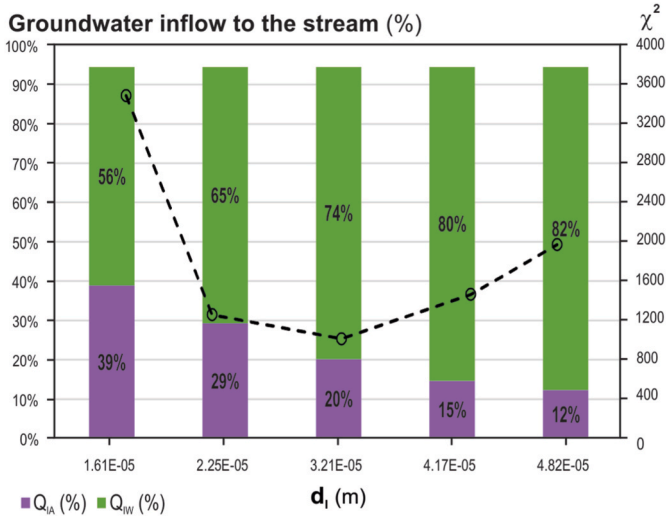


**Fig. 9.** Impact of the thickness of the diffusive layer on the distribution of groundwater fluxes and on the fitting of the modeling approach illustrated by the $\chi^2$.

assumed to be 0), whereas their $NO_3^-$ concentrations vary along the stream (*i.e.* from 0 to 41 mg/L, Table 3). Although the dilution process by interflows appears to be the dominant process to explain this evolution, the rapid decrease of $PO_4^{3-}$ could also be due to adsorption on streambed sediments (Thompson et al., 2011; Wu et al., 2021).

The variability in $NO_3^-$ concentrations in groundwater interflow from the riparian wetlands could be attributed to (i) the variability of the groundwater quality upstream the wetlands or (ii) the variability of biochemical processes occurring in wetlands that affect the quality of water. The groundwater quality upstream of the wetlands can be due to the range of residence times from the top to the base of the saturated sand aquifer (Corcho Alvarado et al., 2009). It is assumed that nutrient pollution of the groundwater from intensive agriculture is relatively recent while groundwater, with mean residence times longer than 100 years (*i.e.* older than the development of intensive agriculture), is less impacted by nutrients inputs. Due to the topographic gradient, riparian wetlands drain deeper parts of the aquifer from upstream to downstream. The portion of groundwater that sustains the wetlands is thus more recent and enriched in nutrients in the upstream part of the catchment than in the downstream part. Another explanation of this variability could be the diversity of land uses in the watershed. Agricultural zones (mainly traditional, with less than 2.5 % of the area managed with organic practices), developed rural areas (with road networks and private yards or gardens), urban areas, and natural zones leach different amounts of nutrients and pollutants into groundwater (Billen et al., 2007b; Garnier et al., 2014). The two samples of groundwater from wetlands with the highest contents of $NO_3^-$ are the nearest to the agricultural area in the northeastern side of the catchment. Therefore, the variability of groundwater quality at the outlet of riparian wetlands can be due to a combination of these two factors.

In riparian wetlands, $NO_3^-$ concentrations can decrease in water due to processes such as plants assimilation and denitrification (Barnaud and Fustec, 2007; Martinez-Espinosa et al., 2021). The large range of denitrification rates within wetlands reported in the literature is explained by the variability of wetlands properties and structures, such as organic matter contents and hydraulic conductivity (Hattermann et al., 2006). The best conditions for high denitrification rates are (i) anaerobic conditions, (ii) pH values between 5.5 and 8, and (iii) a large amount of electron donors as organic matter (Rivett et al., 2008). Moreover, the slower the transit of the water in the wetland is, the higher is the removal of $NO_3^-$. In wetlands where there are many ditches that channelized groundwater springs, the efficiency of $NO_3^-$ removal decreases (Ranalli and Macalady, 2010). In this study, due to a too short transit time of the water in the ditches, interflows seem not to be inflected by denitrification: with a mean concentration of 21 mg $NO_3^-$/L at the outlet of the ditches, riparian interflows cannot improve the N-quality of the stream.

The evolution of stream water quality could also be explained by processes in the hyporheic zone. The results obtained with the ceramic cups samples divide the Rhodon stream in two parts, above 3 km and below 3 km. In the upper area, the high $NO_3^-$ concentrations in groundwater inflow from the aquifer can be explained by the local pollution of groundwater in the streambed induced by effluent loss from the WWTP upstream. Downstream, $NO_3^-$ concentrations in the streambed are lower than 5 mg/L while in the local area of the study site, the mean content in $NO_3^-$ in the aquifer was around 30 mg/L in 2004 (Schneider, 2005). The decrease of $NO_3^-$ in the streambed could be the result of hyporheic processes. Many studies have shown that denitrification can occur in the hyporheic zone (Buss et al., 2009; Harvey et al., 2013; Zarnetske et al., 2011) and that hyporheic exchange with stream water can be much higher than exchanges between groundwater and stream water (see review of Cranswick and Cook, 2015). Vertical profiles within the streambed, such as described by Cranswick et al. (2014), could help to solve this issue. At this state, the sampling in the streambed was suitable to constrain groundwater chemistry for the mass balance approach because it integrates hyporheic processes occurring along the stream that impact groundwater quality although they are not considered in the equations.

### 5.3. Recommendations and perspectives

In this work, the methods and tools used were calibrated to better understand the groundwater-stream interaction with the best balance between the field work, the uncertainties of data and the uncertainties of the modelling approach. The approach does not assess precisely the processes occurring in wetlands or in hyporheic zone but gives a good estimation of water fluxes and allows a rapid understanding of the dynamic of the catchment.

The modeling approach could be improved by testing some of the underlying assumptions and implementing complementary investigations. For example, the assumed constant velocity of diffusion could be better validated by using an artificial tracer test, such as $SF_6$ injection (Cook et al., 2006) or Xe injection (Avery et al., 2018) to combine with the $^{222}Rn$ measurements in the stream. However, an uncertainty remains depending on the method used to analyze these gases. Results of an inter-laboratory comparison of tracer analyses for dating groundwater performed on boreholes located in the Rhodon catchment in 2012 show high $SF_6$ amounts in groundwater (Labasque et al., 2014). Thus, this complementary test could not improve the accuracy of the modeling approach.

Since the results show that the main part of groundwater inflow comes from riparian wetlands, another source of uncertainty is the part of interflow that transits through the wetland sediments (*i.e.* subsurface inflows). In this work, it was assumed that this flow was negligible because of the low hydraulic conductivity of the sediments and the large amount of surface flow from the wetlands. However, if the subsurface flow path becomes significant, the modeling results could be affected, in catchment where the wetlands sediments could be enriched in $^{226}Ra$. In that specific case, the $^{222}Rn$ activity of wetland subsurface flows could be higher than the one from the surface (Gilfedder et al., 2015). It will decrease the estimation of the groundwater flow coming from the aquifer to increase the impact of riparian wetland on groundwater fluxes. Thus, it would be useful to instrument a riparian wetland with mini piezometers to estimate sediment hydraulic conductivity and $^{222}Rn$ activity, and to model a range of possible contributions to the subsurface inflows in the total interflows. This future work would help to define more accurately how groundwater interacts with the riparian wetlands in small headwater catchments such as the Rhodon watershed.

Finally, the understanding of the flow dynamic in the catchment presented in this paper could allow to investigate more the nitrate dynamic in the stream in the next study. To achieve this new objective, complementary data should be collected such as other nitrogen species ($NH_4^+$, $NO_2^-$), dissolved oxygen and $\delta^{15}N_{NO_3^-}$ for each water reservoir: the groundwater beneath the streambed, the interflows from wetlands, and the stream.

## 6. Conclusion

The objectives of this research were (i) to expand the use of $^{222}Rn$ as a groundwater tracer for small streams in headwater catchments to distinguish groundwater flows received directly from the aquifer and from riparian wetlands and (ii) to characterize the impact of the groundwater flow pathways on the stream quality. Because of their importance in water resource management and in pollution prevention, the quantification of groundwater discharge through wetlands and the distinction of the different flow paths are essential. A $^{222}Rn$ mass balance model was used to differentiate the two different groundwater flow paths (groundwater flows from the aquifer and interflows from wetlands), and to calculate their respective proportions in a small headwater catchment located south of Paris (France). This approach was completed with the assessment of nutrients ($PO_4^{3-}$ and $NO_3^-$) spatial

distributions to highlight the role of groundwater flow paths on the evolution of stream quality.

The combination of stream flows and $^{222}Rn$ activities provides an insight into surface groundwater interflow from wetlands and groundwater inflow from the aquifer to the stream with a satisfactory spatial resolution. The results show that around 80 % of groundwater inflow to the Rhodon stream comes from interflows from wetlands. It is demonstrated that wetlands are of great importance for stream flow quality but with variable effect, likely due to the spatial distribution of groundwater age in upstream wetlands, and to the variation of surface and subsurface flow proportions in wetlands. These results illustrate the complexity of water and nutrient dynamics in a headwater catchment area, despite its small size and relatively simple geology.

This study shows the importance of constraining groundwater flow paths to manage watersheds from small to large scales. Some issues remain to be addressed in quantifying the proportion of subsurface flows in wetlands, where contaminant concentrations can be attenuated by redox processes such as denitrification. However, the method presented here is accurate enough to evaluate the distribution of groundwater flow paths between aquifer and wetlands and prove that with a minimum of data collection, the comprehension of the catchment dynamic is satisfying. Moreover, the tools used are very easy to apply to any catchment and could be useful in all other small headwater streams where the bimodal discharge of groundwater is related to the presence of multiple riparian wetlands. Better estimation of the importance of groundwater flowing in riparian wetland will help to protect these ecosystem and water quality.

## CRediT authorship contribution statement

**K. Lefebvre:** Writing – original draft, Validation, Software, Resources, Methodology, Investigation, Formal analysis, Data curation, Conceptualization. **F. Barbecot:** Writing – original draft, Supervision, Methodology, Funding acquisition, Conceptualization. **M. Larocque:** Writing – original draft, Validation, Supervision, Software, Methodology, Conceptualization. **E. Gibert-Brunet:** Writing – original draft, Supervision. **M. Gillon:** Writing – original draft, Supervision, Methodology, Investigation, Conceptualization. **A. Noret:** Writing – original draft, Methodology, Investigation. **C. Delbart:** Writing – original draft, Methodology, Investigation.

## Declaration of competing interest

The authors declare that they have no known competing financial interests or personal relationships that could have appeared to influence the work reported in this paper.

## Data availability

Data will be made available on request.

## Acknowledgements

The authors would like to thank the French National Association of Research and Technology (ANRT) and the Regional Natural Park of the Haute Vallée de Chevreuse (PNRHVC) for their financial support of this work. The members of the nature and environment team of the park are also thanked for their technical support and their help during the fieldwork. The authors would like to thank Léonora Fleurent of the GEOPS laboratory for her help during field and analytical works. Finally, they would like to thank the two reviewers for their helpful comments.

## References

Adams, R.K., Spotila, J.A., 2005. The form and function of headwater streams based on field and modeling investigations in the southern Appalachian Mountains. Earth Surf. Process. Landforms 30 (12), 1521–1546. https://doi.org/10.1002/esp.1211.

Adyasari, D., Dimova, N.T., Dulai, H., Gilfedder, B.S., Cartwright, I., McKenzie, T., , et al. Fuleky, P., 2023. Radon-222 as a groundwater discharge tracer to surface waters. Earth Sci. Rev. 238 https://doi.org/10.1016/j.earscirev.2023.104321.

Alard, D., 2002. Zones humides de la basse vallée de la Seine. Programme Scientifique Seine Aval, Ifremer, Agence de l'Eau Seine Normandie et Région Haute Normandie 15, 1–36. Rouen, France.

Alexander, R.B., Boyer, E.W., Smith, R.A., Schwarz, G.E., , et al.Moore, R.B., 2007. The role of headwater streams in downstream water quality. J. Am. Water Resour. Assoc. 43 (1), 41–59. https://doi.org/10.1111/j.1752-1688.2007.00005.x.

Atkins, M.L., Santos, I.R., , et al.Maher, D.T., 2016. Assessing groundwater-surface water connectivity using radon and major ions prior to coal seam gas development (Richmond River Catchment, Australia). Appl. Geochem. 73, 35–48. https://doi.org/10.1016/j.apgeochem.2016.07.012.

Atkinson, A.P., Cartwright, I., Gilfedder, B.S., Hofmann, H., Unland, N.P., Cendón, D.I., , et al.Chisari, R., 2015. A multi-tracer approach to quantifying groundwater inflows to an upland river; assessing the influence of variable groundwater chemistry. Hydrol. Process. 29 (1), 1–12. https://doi.org/10.1002/hyp.10122.

Avery, E., Bibby, R., Visser, A., Esser, B., , et al.Moran, J., 2018. Quantification of groundwater discharge in a subalpine stream using radon-222. Water 10 (2), 100. https://doi.org/10.3390/w10020100.

Barbecot, F., 2006. Etude du fonctionnement hydrologique d'un petit bassin versant. Vallée du Rhodon. Parc naturel Régional de la Haute Vallée de Chevreuse. Rapport d'étude 62pp.

Bariteau, A., 1996. Modélisation géochimique d'un aquifère: la nappe de l'Oligocène en Beauce et l'altération des Sables de Fontainebleau.

Barnaud, G., Fustec, E., 2007. Conserver les milieux humides: pourquoi? comment? *Quae/Educagri editions*, 296pp.

Batlle-Aguilar, J., Harrington, G.A., Leblanc, M., Welch, C., , et al.Cook, P.G., 2014a. Chemistry of groundwater discharge inferred from longitudinal river sampling. Water Resour. Res. 50 (2), 1550–1568. https://doi.org/10.1002/2013wr013591.

Batlle-Aguilar, J., Harrington, G., Leblanc, M., Welch, C., et Cook, P., 2014b. Chemistry of groundwater discharge inferred from longitudinal river sampling. Water Resour. Res. 50 (2), 1550–1568.

Becker, M.W., Georgian, T., Ambrose, H., Siniscalchi, J., , et al.Fredrick, K., 2004. Estimating flow and flux of ground water discharge using water temperature and velocity. J. Hydrol. 296 (1–4), 221–233. https://doi.org/10.1016/j.jhydrol.2004.03.025.

Bieroza, M., Hallberg, L., Livsey, J., Prischl, L.A., , et al.Wynants, M., 2024. Recognizing agricultural headwaters as critical ecosystems. Environ. Sci. Technol. 58 (11), 4852–4858. https://doi.org/10.1021/acs.est.3c10165.

Billen, G., Garnier, J., Mouchel, J.M., , et al.Silvestre, M., 2007a. The Seine system: introduction to a multidisciplinary approach of the functioning of a regional river system. Sci. Total Environ. 375 (1–3), 1–12. https://doi.org/10.1016/j.scitotenv.2006.12.001.

Billen, G., Garnier, J., Nemery, J., Sebilo, M., Sferratore, A., Barles, S., Benoit, M., 2007b. A long-term view of nutrient transfers through the Seine river continuum. Sci. Total Environ. 375 (1–3), 80–97. https://doi.org/10.1016/j.scitotenv.2006.12.005.

Billen, G., Ramarson, A., Thieu, V., Théry, S., Silvestre, M., Pasquier, C., Garnier, J., 2018. Nitrate retention at the river–watershed interface: a new conceptual modeling approach. Biogeochemistry 139 (1), 31–51. https://doi.org/10.1007/s10533-018-0455-9.

Boulton, A.J., Datry, T., Kasahara, T., Mutz, M., , et al.Stanford, J.A., 2010. Ecology and management of the hyporheic zone: stream–groundwater interactions of running waters and their floodplains. J. North Am. Benthol. Soc. 29 (1), 26–40. https://doi.org/10.1899/08-017.1.

BRGM, 1975. Carte géologique au 1/50000, vol. 218. Feuille de Rambouillet.

Briggs, M.A., Lautz, L.K., , et al.McKenzie, J.M., 2012. A comparison of fibre-optic distributed temperature sensing to traditional methods of evaluating groundwater inflow to streams. Hydrol. Process. 26 (9), 1277–1290. https://doi.org/10.1002/hyp.8200.

Broecker, W.S., Peng, T.-H., 1974. Gas exchange rates between air and sea. Tellus XXVI.

Bullock, A., Acreman, M., 2003. The role of wetlands in the hydrological cycle. Hydrol. Earth Syst. Sci. Discuss. 7 (3), 358–389.

Buss, S., Cai, Z., Cardenas, B., Fleckenstein, J.H., Hannah, D.M., Heppell, K., Kaeser, D., 2009. The Hyporheic Handbook.

Büttner, G., Kosztra, B., 2007. CLC2006 Technical Guidelines, p. 45pp. European Environment Agency, Technical Report n°17.

Cable, J.E., Burnett, W.C., Chanton, J.P., , et al.Weatherly, G.L., 1996. Estimating groundwater discharge into the northeastern Gulf of Mexico using radon-222. Earth Planet Sci. Lett. 144 (3), 591–604.

Cartwright, I., et Gilfedder, B., 2015. Mapping and quantifying groundwater inflows to Deep Creek (Maribyrnong catchment, SE Australia) using 222Rn, implications for protecting groundwater-dependant ecosystems. Appl. Geochem. 52, 118–129. https://doi.org/10.1016/j.apgeochem.2014.11.020.

Cartwright, I., Hofmann, H., Sirianos, M.A., Weaver, T.R., et Simmons, C.T., 2011. Geochemical and 222Rn constraints on baseflow to the Murray River, Australia, and timescales for the decay of low-salinity groundwater lenses. J. Hydrol. 405 (3–4), 333–343. https://doi.org/10.1016/j.jhydrol.2011.05.030.

Constantz, J., 2008. Heat as a tracer to determine streambed water exchanges. Water Resour. Res. 44 (4), 1–20. https://doi.org/10.1029/2008wr006996. W00D10.

Cook, P.G., 2013. Estimating groundwater discharge to rivers from river chemistry surveys. Hydrol. Process. 27 (25), 3694–3707. https://doi.org/10.1002/hyp.9493.
Cook, P.G., Favreau, G., Dighton, J.C., , et al.Tickell, S., 2003. Determining natural groundwater influx to a tropical river using radon, chlorofluorocarbons and ionic environmental tracers. J. Hydrol. 277 (1–2), 74–88. https://doi.org/10.1016/s0022-1694(03)00087-8.
Cook, P.G., Lamontagne, S., Berhane, D., Clark, J.F., et al., 2006. Quantifying Groundwater Discharge to Cockburn River, Southeastern Australia, Using Dissolved Gas Tracers 222Rn and SF6. *Water Resources Research, 42*(10). doi: 10.1029/2006wr004921.
Corcho Alvarado, J.A., Purtschert, R., Barbecot, F., Chabault, C., Rueedi, J., Schneider, V., Loosli, H.H., 2007a. Constraining the age distribution of highly mixed groundwater using39Ar: a multiple environmental tracer (3H/3He,85Kr,39Ar, and14C) study in the semiconfined Fontainebleau Sands Aquifer (France). Water Resour. Res. 43 (3), 1–16. https://doi.org/10.1029/2006wr005096. W03427.
Corcho Alvarado, J.A., Purtschert, R., Barbecot, F., Chabault, C., Rueedi, J., Schneider, V., Loosli, H.H., 2007b. Constraining the age distribution of highly mixed groundwater using39Ar: a multiple environmental tracer (3H/3He,85Kr,39Ar, and14C) study in the semiconfined Fontainebleau Sands Aquifer (France). Water Resour. Res. 43 (3) https://doi.org/10.1029/2006wr005096.
Corcho Alvarado, J.A., Barbecot, F., et Purtschert, R., 2009. Ambient vertical flow in long-screen wells: a case study in the Fontainebleau Sands Aquifer (France). Hydrogeol. J. 17 (2), 425–431. https://doi.org/10.1007/s10040-008-0383-1.
Craig, H., 1957. Isotopic standards for carbon and oxygen and correction factors for mass-spectrometric analysis of carbon dioxide. Geochem. Cosmochim. Acta 12 (1–2), 133–149. https://doi.org/10.1016/0016-7037(57)90024-8.
Cranswick, R.H., Cook, P.G., 2015. Scales and magnitude of hyporheic, river-aquifer and bank storage exchange fluxes. Hydrol. Process. 29 (14), 3084–3097. https://doi.org/10.1002/hyp.10421.
Cranswick, R.H., Cook, P.G., , et al.Lamontagne, S., 2014. Hyporheic zone exchange fluxes and residence times inferred from riverbed temperature and radon data. J. Hydrol. 519, 1870–1881. https://doi.org/10.1016/j.jhydrol.2014.09.059.
Curie, F., Ducharne, A., Sebilo, M., , et al.Bendjoudi, H., 2009. Denitrification in a hyporheic riparian zone controlled by river regulation in the Seine river basin (France). Hydrol. Process. 23 (5), 655–664. https://doi.org/10.1002/hyp.7161.
Dick, J.J., Tetzlaff, D., , et al.Soulsby, C., 2017. Role of riparian wetlands and hydrological connectivity in the dynamics of stream thermal regimes. Nord. Hydrol, nh2017066. https://doi.org/10.2166/nh.2017.066.
Dulaiova, H., Peterson, R.N., Burnett, W.C., , et al.Lane-Smith, D., 2005. A multi-detector continuous monitor for assessment of 222Rn in the coastal ocean. J. Radioanal. Nucl. Chem. 263 (2), 361–365.
Fabre, C., Sauvage, S., Guilhen, J., Cakir, R., Gerino, M., , et al.Sánchez-Pérez, J.M., 2020. Daily denitrification rates in floodplains under contrasting pedo-climatic and anthropogenic contexts: modelling at the watershed scale. Biogeochemistry 149 (3), 317–336. https://doi.org/10.1007/s10533-020-00677-4.
Fritz, K.M., Schofield, K.A., Alexander, L.C., McManus, M.G., Golden, H.E., Lane, C.R., Pollard, A.I., 2018. Physical and chemical connectivity of streams and riparian wetlands to downstream waters: a synthesis. J. Am. Water Resour. Assoc. 54 (2), 323–345. https://doi.org/10.1111/1752-1688.12632.
Garnier, J., Billen, G., Vilain, G., Benoit, M., Passy, P., Tallec, G., Kao, C., 2014. Curative vs. preventive management of nitrogen transfers in rural areas: lessons from the case of the Orgeval watershed (Seine River basin, France). J. Environ. Manag. 144, 125–134. https://doi.org/10.1016/j.jenvman.2014.04.030.
Gilfedder, B.S., Frei, S., Hofmann, H., , et al.Cartwright, I., 2015. Groundwater discharge to wetlands driven by storm and flood events: quantification using continuous Radon-222 and electrical conductivity measurements and dynamic mass-balance modelling. Geochem. Cosmochim. Acta 165, 161–177. https://doi.org/10.1016/j.gca.2015.05.037.
Gillon, M., Barbecot, F., Gibert, E., Corcho Alvarado, J.A., Marlin, C., , et al.Massault, M., 2009. Open to closed system transition traced through the TDIC isotopic signature at the aquifer recharge stage, implications for groundwater 14C dating. Geochem. Cosmochim. Acta 73 (21), 6488–6501. https://doi.org/10.1016/j.gca.2009.07.032.
Gillon, M., Barbecot, F., Gibert, E., Plain, C., Corcho-Alvarado, J.A., , et al.Massault, M., 2012. Controls on 13C and 14C variability in soil CO2. Geoderma 189–190, 431–441. https://doi.org/10.1016/j.geoderma.2012.06.004.
Gleeson, T., Manning, A.H., Popp, A., Zane, M., , et al.Clark, J.F., 2018. The suitability of using dissolved gases to determine groundwater discharge to high gradient streams. J. Hydrol. 557, 561–572. https://doi.org/10.1016/j.jhydrol.2017.12.022.
Grivel, S., Caessteker, P., 2015. Têtes de bassin versant. Milieux, usages, enjeux et politiques publiques. Têtes de bassin: comment concilier les enjeux sur ces territoires hors du commun? Paris.
Haggard, B.E., Stanley, E.H., , et al.Storm, D.E., 2005. Nutrient retention in a point-source-enriched stream. J. North Am. Benthol. Soc. 24 (1), 29–47. https://doi.org/10.1899/0887-3593(2005)024<0029:Nriaps>2.0.Co;2.
Harvey, J.W., Böhlke, J.K., Voytek, M.A., Scott, D., , et al.Tobias, C.R., 2013. Hyporheic zone denitrification: controls on effective reaction depth and contribution to whole-stream mass balance. Water Resour. Res. 49 (10), 6298–6316. https://doi.org/10.1002/wrcr.20492.
Hattermann, F.F., Krysanova, V., Habeck, A., , et al.Bronstert, A., 2006. Integrating wetlands and riparian zones in river basin modelling. Ecol. Model. 199 (4), 379–392. https://doi.org/10.1016/j.ecolmodel.2005.06.012.
Kalin, L., Hantush, M., Isik, S., Yucekaya, A., et Jordan, T., 2012. Nutrient Dynamics in flooded wetlands. II: model application. J. Hydrol. Eng. 18 (12), 1724–1738.
Khamis, K., Blaen, P.J., Comer-Warner, S., Hannah, D.M., MacKenzie, A.R., , et al. Krause, S., 2021. High-frequency monitoring reveals multiple frequencies of nitrogen and carbon mass balance dynamics in a headwater stream. Frontiers in Water 3. https://doi.org/10.3389/frwa.2021.668924.
Labasque, T., Aquilina, L., Vergnaud, V., Hochreutener, R., Barbecot, F., , et al.Casile, G., 2014. Inter-comparison exercises on dissolved gases for groundwater dating – (1) Goals of the exercise and site choice, validation of the sampling strategy. Appl. Geochem. 40, 119–125. https://doi.org/10.1016/j.apgeochem.2013.11.007.
Landon, M.K., Rus, D.L., et Harvey, F.E., 2001. Comparison of instream methods for measuring hydraulic conductivity in sandy streambeds. Groundwater 39 (6), 870–885. https://doi.org/10.1111/j.1745-6584.2001.tb02475.x.
Lane, C.R., Creed, I.F., Golden, H.E., Leibowitz, S.G., Mushet, D.M., Rains, M.C., Vanderhoof, M.K., 2022. Vulnerable waters are essential to watershed resilience. Ecosystems 26, 1–28. https://doi.org/10.1007/s10021-021-00737-2.
Larocque, M., Biron, P.M., Buffin-Bélanger, T., Needelman, M., Cloutier, C.-A., , et al. McKenzie, J.M., 2016. Role of the geomorphic setting in controlling groundwater–surface water exchanges in riverine wetlands: a case study from two southern Québec rivers (Canada). Can. Water Resour. J./Revue canadienne des ressources hydriques. https://doi.org/10.1080/07011784.2015.1128360 (in press).
Lefebvre, K., 2015. Diagnostic et quantification des flux nappe - rivière : modélisations hydrodynamique et géochimique du bassin versant de l'Yvette amont (France). Sciences de la Terre. Université Paris Saclay (COmUE); Université du Québec à Montréal. NNT : 2015SACLS152 . tel01287173).
Lefebvre, K., Barbecot, F., Ghaleb, B., Larocque, M., , et al.Gagne, S., 2013. Full range determination of (2)(2)(2)Rn at the watershed scale by liquid scintillation counting. Appl. Radiat. Isot. 75, 71–76. https://doi.org/10.1016/j.apradiso.2013.01.027.
Lefebvre, K., Barbecot, F., Larocque, M., et Gillon, M., 2015. Combining isotopic tracers (222Rn and δ13C) for improved modelling of groundwater discharge to small rivers. Hydrol. Process. 29 (12), 2814–2822. https://doi.org/10.1002/hyp.10405.
Marti, E., Aumatell, J., Godé, L., Poch, M., et Sabater, F., 2004. Nutrient retention efficiency in streams receiving inputs from wastewater treatment plants. J. Environ. Qual. 33 (1), 285–293.
Martinez, J.L., Raiber, M., , et al.Cox, M.E., 2015. Assessment of groundwater–surface water interaction using long-term hydrochemical data and isotope hydrology: headwaters of the Condamine River, Southeast Queensland, Australia. Sci. Total Environ. 536, 499–516.
Martinez-Espinosa, C., Sauvage, S., Al Bitar, A., Green, P.A., Vorosmarty, C.J., , et al. Sanchez-Perez, J.M., 2021. Denitrification in wetlands: a review towards a quantification at global scale. Sci. Total Environ. 754, 142398 https://doi.org/10.1016/j.scitotenv.2020.142398.
Marx, A., Dusek, J., Jankovec, J., Sanda, M., Vogel, T., van Geldern, R., Barth, J.A.C., 2017. A review of CO2 and associated carbon dynamics in headwater streams: a global perspective. Rev. Geophys. 55 (2), 560–585. https://doi.org/10.1002/2016rg000547.
McCallum, J.L., Cook, P.G., Berhane, D., Rumpf, C., et McMahon, G.A., 2012. Quantifying groundwater flows to streams using differential flow gaugings and water chemistry. J. Hydrol. 416–417, 118–132. https://doi.org/10.1016/j.jhydrol.2011.11.040.
Ménillet, F., 1988. Meulières, argiles à meulières et meuliérisation: historique, évolution des termes et hypothèses génétiques [Meulières, Clay meulières and meuliérisation: historical evolution of the terms and assumptions genetic]. Bull. Inf. Geol. Bassin Paris 25 (4), 71–79.
Meredith, E.L., Kuzara, S.L., 2012. Identification and quantification of base flow using carbon isotopes. Ground Water 50 (6), 959–965. https://doi.org/10.1111/j.1745-6584.2012.00952.x.
Meredith, K.T., Hollins, S.E., Hughes, C.E., Cendón, D.I., Hankin, S., et Stone, D.J.M., 2009. Temporal variation in stable isotopes (18O and 2H) and major ion concentrations within the Darling River between Bourke and Wilcannia due to variable flows, saline groundwater influx and evaporation. J. Hydrol. 378 (3–4), 313–324. https://doi.org/10.1016/j.jhydrol.2009.09.036.
Météo_France, 2014. Données climatologiques de la station de Trappes, vol. 78.
Meyer, J.L., Strayer, D.L., Wallace, J.B., Eggert, S.L., Helfman, G.S., , et al.Leonard, N.E., 2007. The contribution of headwater streams to biodiversity in river Networks1. JAWRA Journal of the American Water Resources Association 43 (1), 86–103. https://doi.org/10.1111/j.1752-1688.2007.00008.x.
Molenat, J., Gascuel-Odoux, C., Ruiz, L., , et al.Gruau, G., 2008. Role of water table dynamics on stream nitrate export and concentration in agricultural headwater catchment (France). J. Hydrol. 348 (3–4), 363–378. https://doi.org/10.1016/j.jhydrol.2007.10.005.
Moore, R., 2004a. Introduction to salt dilution gauging for streamflow measurement Part 2: constant-rate injection. Streamline Watershed Management Bulletin 8 (1), 11–15.
Moore, R., 2004b. Introduction to salt dilution gauging for streamflow measurement: Part 1. Streamline Watershed Management Bulletin 7 (4), 20–23.
Oh, Y.H., Koh, D.-C., Kwon, H.-I., Jung, Y.-Y., Lee, K.Y., Yoon, Y.-Y., Ha, K., 2021. Identifying and quantifying groundwater inflow to a stream using 220Rn and 222Rn as natural tracers. J. Hydrol.: Reg. Stud. 33 https://doi.org/10.1016/j.ejrh.2021.100773.
Peyrard, D., Delmotte, S., Sauvage, S., Namour, P., Gerino, M., Vervier, P., , et al. Sanchez-Perez, J.M., 2011. Longitudinal transformation of nitrogen and carbon in the hyporheic zone of an N-rich stream: a combined modelling and field study. Phys. Chem. Earth, Parts A/B/C 36 (12), 599–611. https://doi.org/10.1016/j.pce.2011.05.003.
Rampon, G., 1965. Etat de la documentation sur les ouvrages souterrains implantés sur les feuilles topographiques de Nogent le Roi-Rambouillet et synthèse hydrogéologique provisoire [State of the documentation on the underground Structures located on the leaves topographic Nogent le-Roi-Rambouillet and provisional hydrogeological synthesis]. Rapport du BRGM DSGR 65, A7.

Ranalli, A.J., Macalady, D.L., 2010. The importance of the riparian zone and in-stream processes in nitrate attenuation in undisturbed and agricultural watersheds – a review of the scientific literature. J. Hydrol. 389 (3–4), 406–415. https://doi.org/10.1016/j.jhydrol.2010.05.045.

Rivett, M.O., Buss, S.R., Morgan, P., Smith, J.W., , et al.Bemment, C.D., 2008. Nitrate attenuation in groundwater: a review of biogeochemical controlling processes. Water Res. 42 (16), 4215–4232. https://doi.org/10.1016/j.watres.2008.07.020.

Schmadel, N.M., Ward, A.S., , et al.Wondzell, S.M., 2017. Hydrologic controls on hyporheic exchange in a headwater mountain stream. Water Resour. Res. 53 (7), 6260–6278. https://doi.org/10.1002/2017wr020576.

Schneider, V., 2005. Apports de l'hydrodynamique et de la géochimie à la caractérisation des nappes de l'Oligocène et de l'Éocène, et à la reconnaissance de leurs relations actuelles et passées : origine de la dégradation de la nappe de l'Oligocène (sud-ouest du Bassin de Paris). Université Paris Sud 11, 298pp.

Schubert, M., Siebert, C., Knoeller, K., Roediger, T., Schmidt, A., , et al.Gilfedder, B., 2020. Investigating groundwater discharge into a major river under low flow conditions based on a radon mass balance supported by tritium data. Water 12 (10). https://doi.org/10.3390/w12102838.

Smerdon, B.D., Payton Gardner, W., Harrington, G.A., , et al.Tickell, S.J., 2012. Identifying the contribution of regional groundwater to the baseflow of a tropical river (Daly River, Australia). J. Hydrol. 464–465, 107–115. https://doi.org/10.1016/j.jhydrol.2012.06.058.

Sophocleous, M., 2002. Interactions between groundwater and surface water: the state of the science. Hydrogeol. J. 10 (1), 52–67. https://doi.org/10.1007/s10040-001-0170-8.

Staponites, L.R., Bartak, V., Bily, M., et Simon, O.P., 2019. Performance of landscape composition metrics for predicting water quality in headwater catchments. Sci. Rep. 9 (1), 14405 https://doi.org/10.1038/s41598-019-50895-6.

Stellato, L., Petrella, E., Terrasi, F., Belloni, P., Belli, M., Sansone, U., , et al.Celico, F., 2008. Some limitations in using 222Rn to assess river–groundwater interactions: the case of Castel di Sangro alluvial plain (central Italy). Hydrogeol. J. 16 (4), 701–712. https://doi.org/10.1007/s10040-007-0263-0.

Tetzlaff, D., Birkel, C., Dick, J., Geris, J., , et al.Soulsby, C., 2014. Storage dynamics in hydropedological units control hillslope connectivity, runoff generation, and the evolution of catchment transit time distributions. Water Resour. Res. 50 (2), 969–985. https://doi.org/10.1002/2013WR014147.

Thompson, S.E., Basu, N.B., Lascurain, J., Aubeneau, A., et Rao, P.S.C., 2011. Relative dominance of hydrologic versus biogeochemical factors on solute export across impact gradients. Water Resour. Res. 47 (10) https://doi.org/10.1029/2010wr009605.

Uchida, T., Asano, Y., Onda, Y., , et al.Miyata, S., 2005. Are headwaters just the sum of hillslopes? Hydrol. Process. 19 (16), 3251–3261. https://doi.org/10.1002/hyp.6004.

Van Stempvoort, D.R., MacKay, D.R., Collins, P., et Koehler, G., 2022. Nutrient delivery by groundwater discharge to headwater streams in agricultural catchments. Hydrol. Process. 36 (10) https://doi.org/10.1002/hyp.14724.

Walton, C.R., Zak, D., Audet, J., Petersen, R.J., Lange, J., Oehmke, C., Hoffmann, C.C., 2020. Wetland buffer zones for nitrogen and phosphorus retention: impacts of soil type, hydrology and vegetation. Sci. Total Environ. 727, 138709 https://doi.org/10.1016/j.scitotenv.2020.138709.

Wang, H., Jiang, X.-W., Wan, L., Han, G., , et al.Guo, H., 2015. Hydrogeochemical characterization of groundwater flow systems in the discharge area of a river basin. J. Hydrol. 527, 433–441. https://doi.org/10.1016/j.jhydrol.2015.04.063.

Weyer, C., Peiffer, S., , et al.Lischeid, G., 2018. Stream water quality affected by interacting hydrological and biogeochemical processes in a riparian wetland. J. Hydrol. 563, 260–272. https://doi.org/10.1016/j.jhydrol.2018.05.067.

Winter, T.C., 1999. Relation of streams lakes and wetlands to groundwater flow systems. Hydrogeol. J. 7, 28–45.

Winter, T.C., Harvey, J.W., Franke, O.L., , et al.Alley, W.M., 1998. Groundwater and Surface Water: a Single Ressource, C1139. US Geological Survey, p. 87pp.

Wipfli, M.S., Richardson, J.S., , et al.Naiman, R.J., 2007. Ecological linkages between headwaters and downstream ecosystems: transport of organic matter, invertebrates, and wood down headwater Channels1. JAWRA Journal of the American Water Resources Association 43 (1), 72–85. https://doi.org/10.1111/j.1752-1688.2007.00007.x.

Wu, S., Tetzlaff, D., Goldhammer, T., , et al.Soulsby, C., 2021. Hydroclimatic variability and riparian wetland restoration control the hydrology and nutrient fluxes in a lowland agricultural catchment. J. Hydrol. 603 https://doi.org/10.1016/j.jhydrol.2021.126904.

Zarnetske, J.P., Haggerty, R., Wondzell, S.M., et Baker, M.A., 2011. Dynamics of nitrate production and removal as a function of residence time in the hyporheic zone. J. Geophys. Res. 116, 1–12. https://doi.org/10.1029/2010jg001356. G01025.

Zhou, Z., Cartwright, I., Morgenstern, U., , et al.Fifield, L.K., 2024. Integrating major ion geochemistry, stable isotopes ((18)O, (2)H) and radioactive isotopes ((222)Rn, (14)C, (36)Cl, (3)H) to understand the interaction between catchment waters and an intermittent river. Sci. Total Environ. 908, 167998 https://doi.org/10.1016/j.scitotenv.2023.167998.